Est. 1984

ORIENTAL JOURNAL OF CHEMISTRY
An International Open Free Access, Peer Reviewed Research Journal

www.orientjchem.org

ISSN: 0970-020 X
CODEN: OJCHEG
2018, Vol. 34, No.(3):
Pg. 1153-1197

Recent Trends in Mussel-Inspired Catechol-Containing Polymers. Part 1 (A Review)

SAAD MOULAY

Laboratoire de Chimie-Physique Moléculaire et Macromoléculaire, Département de Génie des Procédés, Faculté de Technologie, Université Saad Dahlab de Blida, B. P. 270, Route de Soumaa, 09000, Blida, Algeria.
*Corresponding author E-mail: saadmoulay@univ-blida.dz

http://dx.doi.org/10.13005/ojc/340301

(Received: April 03, 2018; Accepted: May 14, 2018)

ABSTRACT

Syntheses and applications of mussel-inspired polymeric materials have gained a foothold in research in recent years. Mussel-inspired chemistry coupled to Michael addition and Schiff's base reactions was the key success for this intensive research. Unequivocally, The basic building brick of these materials is catechol-containing moiety, namely, 3,4-dihydroxyphenyl-L-alanine (L-DOPA or DOPA) and dopamine (DA). These catechol-based units within the chemical structure of the material ensure chiefly its adhesive characteristic to adherends of different natures. The newly-made catechol-bearing polymeric materials exhibit unique features, implying their importance in several uses and applications. Technology advent is being advantaged with these holdfast mussel protein-like materials. This review sheds light into the recent advances of such mussel-inspired materials for their adhesion capacity to several substrata of different natures, and for their applications mainly in antifouling coatings and nanoparticles technology.

Keywords: Adhesion, Antifouling, Catechol, Dopamine, Mussel, Nanoparticles, Polymers.

INTRODUCTION

Nature, such a stunning creature, conceals a plethora of phenomena that serve as models in man's life and procure him solutions for his lingering problems. Such natural phenomena were the background boosting for the development of science as it stands nowadays. Man, an integral part of this huge nature, is himself an astounding creature as he eagerly attempts to understand the natural phenomena, to mimic them, and to set rules and science therefrom. Despite the unprecedented today's commodities, which are the upshots of the science advent, man realizes that Nature remains huge and nearly unchipped, and only a bit of it has been exploited and explored; that is, Nature stands defiantly steadfast and unshakable forever. Yet, it is unfair to deny and scorn what man has so far accomplished for the welfare of his species. Indubitably, he has made a tremendous progress

This is an Open Access article licensed under a Creative Commons Attribution-Non Commercial-Share Alike 4.0 International License (https://creativecommons.org/licenses/by-nc-sa/4.0/), which permits unrestricted Non Commercial use, distribution and reproduction in any medium, provided the original work is properly cited.

towards understanding and unveiling what Nature hides, and adequately exploiting it for his life course. Truly noting, mimicking the nature is not fully successful in many instances.

From this myriad of naturally hidden phenomena, we evoke the astonishing underwater holdfast of marine mussels to hard surfaces. Investigations on such related phenomenon are numerous and have elucidated the fundamental role of L-DOPA (3,4-dihydroxyphenyl-L-alanine) present in the Mytilus foot proteins (*Mfps*) or also called Mytilus adhesive proteins (MAPs)[1-6]. Recently, Mian and Khan[7] provided theoretical evidence for the adhesion of L-DOPA to silica surface through the catechol unit, being able to form four hydrogen bonds as it acts both as a donor and an acceptor of hydrogen. A number of reports have confirmed the synergetic interplay of both catechol unit of L-DOPA and lysine in the adhesion of the mussel to inorganic substrates under wet environment[5,8-11]; while the role of catechol unit in the adhesion process has been well deciphered, that of lysine has not been wholly understood. Yet, Waite *et al.,*[10] advanced that lysine has the function to expel the hydrated cations from the solid surface, making room for catechol to approach the surface. Molecular dynamics simulations study of the adhesion of siderophore analogues bearing lysine, arginine or histidine on ionized silica surface revealed the role of electrostatic interactions in the adhesion mechanism[12]. Moreover, Waite's school[13] proved, by means of cyclic voltammetry and UV-Vis spectroscopy, that at pH ≥7, the quinone form of DOPA actually tautomerizes to α,β-dehydro-DOPA (equation 1); acetate or phosphate anions in the buffers acted as catalyzing Lewis bases. Applying the quartz crystal microbalance (QCM) experiments, the adsorption capacity of α,β-dehydro-DOPA on TiO_2 was found to be 20-fold that of DOPA.

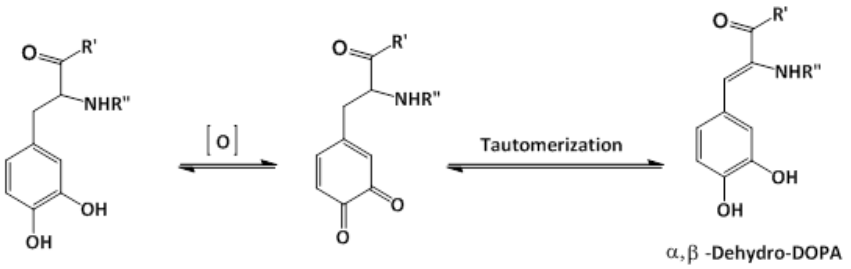

(1)

Wang and his team[14] disclosed results that demonstrate the DOPA proneness to adhere to all surfaces, owing mainly to the aromatic ring or o-hydroxy structure of catechol unit, as the binding to the surface may occur: 1) via o-hydroxy of catechol while the plane of the aromatic ring is perpendicular to the surface, or 2) via aromatic ring of catechol while the plane of the aromatic ring is parallel to the surface. Despite all efforts to elucidate the real mechanism of the aquatic adherence of the *Mfps* and the involved components, other factors remained equally important as recently traced in an elegantly penned and stupendously awesome paper by Waite[15]. With the advent of a deep understanding of the wet bioadhesive phenomenon of *Mfps*, the translation in forms of mussel-inspired materials to biological and biomedical applications has been feasible[16-20]. Chai *et al.,*[21] pointed out that the difference in the sclerotizing and adhesive properties of some natural catecholamines are related to the difference in their reactivities and selectivities towards nucleophiles. Recent Wilker's work[22] has demonstrated the difference in adhesive behavior of the mussel plaques when remained attached and when detached vis-à-vis low- and high-energy surfaces. Contact geometry and plaque shape and its supramolecular architecture were proved to be pivotal in the detachment dynamics which, in turn, played a fundamental role in the adhesion strength[23,24]. Moreover, attempt to understand the biological formation of the plaques from *Mytilus edulis* mussel has given an insight into how to proceed further for designing mussel-inspired polymers for specific applications[25]. A cutting-edge advance in the translation of MAP adhesive property has been the application of polydopamine in cell and tissue engineering[18].

On the other hand, man-made catecholic polymers were reported earlier for their peculiar

chemistry and properties[26-28]. They were prepared either by polymerization of suitable catechol-containing monomers or by chemical modification of polymers with catechol-bearing molecules. Recently, poly(vinylcatechol)s were synthesized via RAFT polymerization (reversible addition-fragmentation chain transfer) of bio-based monomers[29]. By the same polymerization method, poly(vinylgallol), a polyphenol-bioinspired polymer, was made and showed high antioxidant and adsorption properties[30]. Hwang and his co-workers[31] developed a hydrogel based on tunicate-mimetic nanofibrous chitin for wound healing under aquatic conditions; the nanofibrous material was made by reacting chitin with pyrogallol acid. The pyrogallol group is part of 3,4,5-trihydroxyphenylalanine that constitutes the proteins found in tunicates to ensure the wet adhesion. Kurisawa *et al.,*[32] conjugated epigallocatechin-3-gallate, a green tea catechin and a polyphenolic natural substance, to hyaluronic acid. The solution of this conjugate gelled within seven minutes upon addition of horseradish peroxidase (HRP) and at a pH of 7.4; cross-linking within the conjugate system could have taken place in situ through epigallocatechin-3-gallate quinone formation. Numerous mussel-inspired catechol-containing polymers have been realized through well-known polymerizations or chemical functionalizations of a range of polymers, and were shown to be endowed with adhesive property[9,33]. Enzymatic syntheses of catechol-bearing polymeric substances were reviewed[28]. For example, polymerization of catechol in the presence of HRP as catalyst afforded a reddish-brown, water-soluble and electroactive poly(catechol)[34]. Bacteria could be also employed for this aim. For example, Gosset and his co-workers[35] were able to synthesize catechol melanin from glycerol through the use of an engineered *Escherichia coli*.

In this present account, it is intended to survey the sparse investigations linked to mussel-inspired catechol-bearing materials from the year 2015 up to now. This review tackled this issue through the synthetic pathways, in some instances, of these materials and their targeted applications.

The paper is divided into three parts, herein outlined as interrogative subtitles:

1. How adherent are the newly-made mussel-inspired polymers?
2. How good are the anti-fouling properties of mussel-inspired polymeric coatings?
3. How well and useful are the nanoparticles designed with mussel-inspired polymers?

How adherent to substrates are the newly-made mussel-inspired polymers?

Catechol and primary amines in the chemical structures of *Mfps* were disclosed to inherit the wet adhesion of mussels to various substrata[9, 36, 37]. You *et al.,*[38] prepared a set of dopamine analogues with different alkylenic chain lengths between the amine group and catechol unit. They found that these dopamine analogues were able to polymerize with different mechanisms; while propylamine catechol and butylamine catechol polymerized through cyclization followed by oxidative coupling as with dopamine, pentylamine catechol and dodecylamine catechol polymerized in a simple manner, without cyclization. Also, it was proved that the covalent alkenylic linkage was critical to ensure coating ability. However, the alkenylic linkage did not influence the adhesion ability; an adhesive strength of ~90 kPa against glass side in aqueous environment was found for polydopamine and poly(dopamine analogue)s. Furthermore, Lee *et al.,*[39] demonstrated the synergetic effect of catechol and amine groups by comparing the adhesion strength of poly(catecholamine), synthesized by an oxidative polymerization of norepinephrine, with that of polycatechol. To this end, the polymer was placed between two opposing mica surfaces. The coated poly(catecholamine) and polycatechol surfaces presented water contact angles θ_w of 30 and 40°, respectively. The adhesive strength between the poly(catecholamine) layers was about 30 times higher than that for polycatechol layers, 8 h after *in situ* polymerization initiation. This adhesion difference was explained as being due to the number of occurring interactions; that is, while the mechanism of adhesion for poly(catecholamine) included three possible interactions: π-π stacking (the quadrupole-quadrupole interaction of indolic crosslinks), cation-π interaction (the monopole-quadrupole interaction between positively charged amine groups and the indolic crosslinks), and surface salt displacement by the primary amine, that for polycatechol took place only through π-π stacking. However, other related works emphasized that the adhesion property would have stemmed mainly from catechol units[40, 41].

As soon as the bioadhesiveness of mussel feet proteins under wet environment was brought about, several research workers launched studies to comprehend this natural phenomenon[9,11]; indeed, a number of DOPA/catechol-bearing polymers were tested for their adhesiveness to a variety of substrata. Hugel and his co-workers[42] designed a material made of hyperbranched polyglycerol as a hydrophilic core with dopa units attached at the ends of the branches; DOPA entities were covalently attached with a PEG (poly(ethylene glycol)) linker using NHS ester chemistry (NHS = N-hydroxysuccinimide). Such material was examined for its adhesive ability to TiO_2 surfaces using AFM spectroscopy in three aqueous systems: ultrapure water, PBS buffer (and phosphate buffered saline), and McIlvaines buffer solutions at pH 3 (a mixture of 100 mM citric acid and 200 mM Na_2HPO_4). The maximum detachment forces of the adhesive from TiO_2 surfaces were 40, 290, and 410 nN in the three aqueous systems, respectively, under the following conditions: room temperature, pulling velocity of 1 μm s^{-1}, and a surface dwell time of 1 s. Such forces were found to increase with catechol content and with prolonged dwelling time. The lower forces were reasoned in terms of the interaction between the TiO_2 surface and DOPA in oxidized form and the higher ones were due to the unoxidized DOPA; higher pHs promoted the formation of oxidation of catechol units. As to pH effect on the mussel feet protein adhesion to marine surfaces, the work of Waite and his team[43] revealed that an acidic pH (~ 2) is in situ set by the mussel during the plaque formation; the acidic pH has been claimed to delay the auto-oxidation of DOPA residues, enabling the catecholic functionality to form bidentate H-bonds and coordination complexes with substratum surface.

Passerini multicomponent polymerization was employed to realize materials containing pendant catechol units in varying degrees (9 to 70%) as illustrated in equation 2[44]; the multicomponent systems included di-o-nitrobenzaldehyde, 1,6-di-isocyanohexane, 3-(3,4-dihydroxyphenyl) propionic acid, and undecanoic acid. The average molecular weights M_ns and the polydispersity indexes I_ps varied from 6.5 to 14.2 kDa and from 1.59 to 2.76, respectively; the highest M_n was measured for a catechol content of about 23%. The polymer samples with catechol content greater than 60% were of a poor solubility. The decomposition temperatures T_d and the glass transition temperatures T_g were in the range of 249-293 °C and 14.0-70.4 °C, respectively; T_g increased with increasing catechol content. Their adhesion capacity onto a glass plate was quantified by lap shear strength which fluctuated between 0.22 and 0.53 MPa, and this strength, generally, increased with catechol content. These catechol bearing polymers were characterized with the facile ability to degrade upon UV irradiation, that is, a facile detachment from the substrate surface; this photolability was mainly due to the incorporated o-nitrobenzyl ester groups.

Kaneko *et al.,*[45] succeeded in making mussel-inspired plant-derived polymers with terminal catechol units and evaluating their adhesion ability to several substrates. Copolymer of 3,4-dihydroxycinnamic acid (DHCA, caffeic acid) and 4-hydroxycinnamic acid (4HCA, p-coumaric

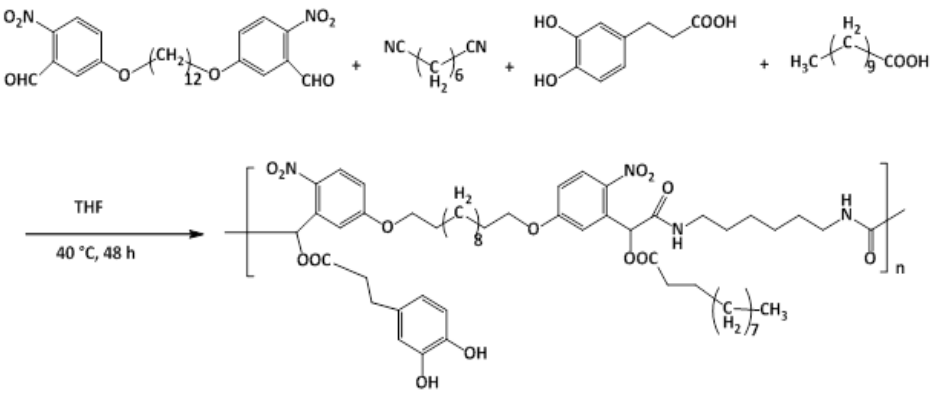

(2)

acid), poly(DHCA-co-4HCA), and copolymer of 4-dihydroxyhydrocinnamic acid (DHHCA) and 3-(3-hydroxyphenyl) propionic acid (3HPPA), poly(DHHCA-co-3HPPA), were achieved via transesterification process using sodium acid phosphate as catalyst. The lap shear adhesion test revealed that poly(DHHCA-co-3HPPA) exhibited the strongest adhesion: 25.60 MPa for glass, 29.60 MPa for carbon, 15.70 MPa for steel, and 16.30 MPa for bovine dentin. That for poly(DHCA-co-4HCA) was respectively: ~9.15, ~8.00, ~4.60, ~6.85 MPa. While the adhesion of poly(DHHCA-co-3HPPA) was superior over the conventional glues (epoxy resin and cyanoacrylate), that of poly(DHCA-co-4HCA) was lower than that of epoxy resin but greater than that of cyanoacrylate glue.

Wilker *et al.,*[41] synthesized *Mfp-mimicking* copolymers of styrene and 3,4-dihydroxystyrene Via anionic polymerization, and compared their underwater adhesion potential to those of commercial glues. The underwater adhesion of the copolymers to aluminum substrate increased from ~0.5 to ~2.5-3 MPa when the molecular weight increased from ~ 2×103 to ~8.5×103 g mol^{-1}, and was maximum for 3,4-dihydroxystyrene content of ~22%; the adhesion declined beyond this catechol content. Adhesion in wet conditions of the commercial glues did not exceed 1 MPa. The lap shear adhesion of copolymer with 28% of 3,4-dihydroxystyrene in deionized water was measured to be 0.4 MPa, but in artificial seawater it was at 1.8 MPa, hinting at the positive role of charges[46]. Besides, a high cytocompatibility of poly[(3,4-dihydroxystyrene)-co-styrene] was demonstrated, suggesting its possible utilization as adhesive for biomedical devices[47]. Wilker's school extended their undertakings on mussel-inspired adhesive polymers to materials containing catechol-bearing poly(lactic acid)[48]. The synthetic strategy involved the oligomerization of 3,4-methylenedioxymandelic acid monomer, followed by melting the obtained oligomer (degree of polymerization of 4-5) into a preformed poly(D,L-lactic acid), a racemic PLA, via a polycondensation reaction catalyzed by $Sn(oct)_2$ (equation 3). Treatment of the obtained copolymer with p-toluenesulfonic acid (TSA) afforded poly[(3,4-dihydroxymandelic acid)-co-(lactic acid)]. The strongest adhesion in air to aluminum, sanded steel, and Teflon substrates was found for a copolymer with molecular weights ranging from ~12 000 to ~34 000 g mol^{-1} and with ~7 mol.% of 3,4-dihydroxymandelic acid and ~93 mol.% of lactic acid. The adhesion strength in air of this biomimetic copolymer in the presence of periodate ion (IO_4^-) against these substrata was 2.6, 1.7, and 0.32 MPa, respectively. These adhesion values were closer to those of Elmer's glue (3, 1.6, and 0.23 MPa, respectively). The copolymer treated with IO_4^- underwent a lower hydrolytic degradation when compared to the untreated one and PLA.

In an effort to establish an interplay of the mechanical properties of adhesive, Meredith and Wilker[49] approached the issue by designing terpolymers made of poly(ethylene glycol) methyl ether methacrylate (PEGMEMA), methyl methacrylate (MMA) and dopamine methacrylamide (DAMAAm) (Fig. 1); these components promoted to the conceived material flexibility, stiffness, and adhesiveness, respectively. The molecular weights

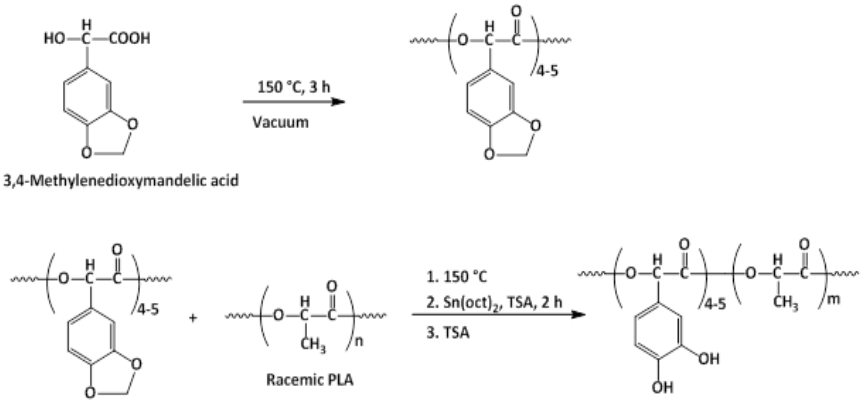

(3)

M_ns of the terpolymers and their I_ps ranged from 5 300 to 24 900 g mol^{-1} and 1.3 to 2.0, respectively. The lap shear adhesion of the terpolymers fluctuated between 0.2 to 2.4 MPa, depending on the contents of the corresponding components. The mechanical properties of the terpolymers varied with varying concentration of three monomer units: elastic modulus from 0.012 to 1.3 GPa, yield strength from 1.1 to 5 MPa, ultimate tensile strength from 2.2 to 7 MPa, and strain from 0.1 to 110%. It was claimed that high PEG content within the material would increase its ductility, weaken its strength, and decrease its adhesion.

Mu and Wan[50] developed a biomimetic adhesive by acetalization poly(vinyl alcohol) with 3,4-dihydroxybenzaldehyde (DHBA), resulting in

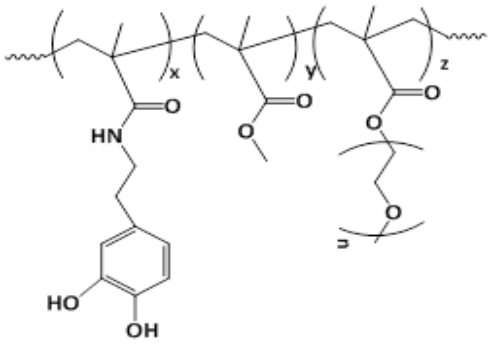

Fig. 1. Poly(PEGMEMA-co-MMA-co-DAMAAm)

poly(vinyl alcohol-g-3,4-dihydroxylbenzyl acetal) (P(VA-g-DHBAc)) with a degree of functionalization of as high as 22.30 mol.% (equation 4). The thus-catechol-functionalized PVA was soluble in DMSO, DMF, NMP, but insoluble in water, chloroform, dichloromethane, methanol, and acetone. Oxidation and crosslinking by air occurred as the yellowish color of the material may have indicated. Such modification disrupted the initial crystallinity of PVA. The tensile strength and elongation at break of P(VA-g-DHBAc) were 12.8 MPa and 250%, respectively, compared to those of virgin PVA (M_w = 67 000 g/mol, Mowiol PVA210), 9.0 and 340%. A bonding strength of the P(VA-g-DHBAc) of about 17.3 MPa on stainless steel surfaces was measured; those of commercial glues, Krazy glue and epoxy glue, were 7.25 and 12.25 MPa, respectively.

Liu and his collaborators[51] fashioned an elastin-like polypeptide (ELP) containing tyrosine, lysine, and valine residues, which was coined the term ELY16. The latter underwent a modification by means of mushroom tyrosinase, converting tyrosines to adhesive DOPA residues in 88%, affording mELY16. The latter protein was found to adsorb to glass at a density nearly twice that of unmodified ELY16, 0.66 µg cm^{-2} against ~0.30 µg cm^{-2}. The lap shear adhesion of mELY16 and ELY16 against aluminum surface in dry environment was 2.1 and 2.6 MPa, respectively, but was 0.24 and 0.05 MPa in humid environment. Both proteins exhibited a good cytocompatibility; about 95% of cell viability was measured.

Catechol-functionalized polyacrylics were prepared by copolymerizing dopamine methacrylamide (DAMAAm) and 2-methoxyethyl methacrylate (MEA) using AIBN as radical initiator [52]. Copolymers with varying catechol contents were obtained by varying the molar ratio of comonomers in the feed, and their molecular weights ranged from 106 700 to 121 800 g mol^{-1} with I_ps of 1.9-2.9. Crosslinking occurred with higher DAMAAm concentration in the feed, as a result of radical scavenging propensity of catechol. Such *in situ* crosslinking led to high mechanical properties

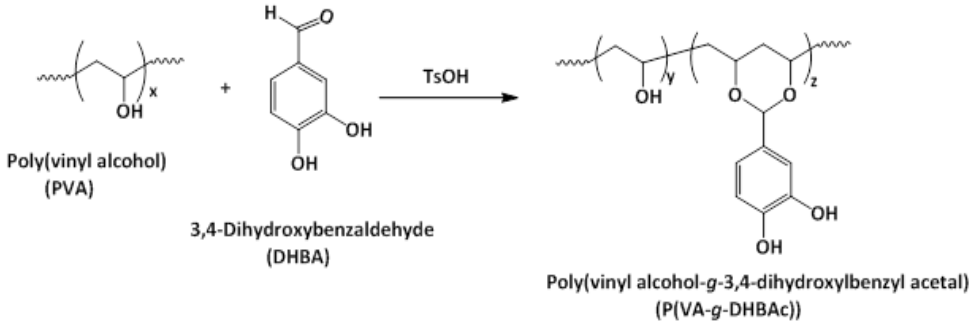

(4)

of the copolymers. For example, the G' and G" of the copolymer with 25% of DAMAAm were 4.8×104 and 3.7×103 kPa, respectively; those for the copolymer with 5% of DAMAAm were only 229 and 84 kPa, respectively. The copolymer with 5% of DAMAAm showed an adhesion strength to glass of about 400 kPa, ~170% higher than that of poly(2-methoxyethyl methacrylate), but those of copolymers with DAMAAm content higher than 5% were surprisingly lower. This finding was imputed to the ensued crosslinking which was verified by oxidizing the copolymer with 5% of DAMAAm with $NaIO_4$. However, the wet adhesion of the copolymers was greater than those of poly(2-methoxyethyl methacrylate) and poly(dopamine methacrylamide), and the lower the DAMAAm content the better the wet adhesion. Overall, the wet adhesion was lower than the dry one.

The adhesive property in wet environment of the mussel-inspired poly[N-(3,4-dihydroxyphenethyl) methacrylamide-co-2-methoxyetheyl acrylate] was cleverly exploited in dentistry, doing away with complications related to saliva[53].

Waite and his team fashioned *Mfp*-mimicking polyelectrolytes and studied their adhesive capacity[54-56]. In their first work[54], they engineered a copolymer mimicking *Mfp-3s*, one of the DOPA-containing protein secreted in the byssus of the marine mussel *Mytilus californianus*; this *Mfp-3s* characterized with a molecular weight of ~ 5 kDa, is able to self-coacervated because of its amphiphilic and ampholytic behavior, and stable to oxidation. The biomimetic copolymer (copolyampholyte) consisted of five randomly arranged comonomer units: a catechol-containing unit, a cationic unit, an anionic unit, a non-ionic hydrophilic (polar) unit, a hydrophobic (polar) unit (Fig. 2). Variations of the latter comonomer units led to an improvement of coacervate formation of the copolyampholyte and its wet adhesion. The cyclic voltammetry profile of the copolyampholyte with 30, 6, 4, 51, and 9% of the respective comonomer units showed an oxidation potential of 0.50 V at pH = 3 and ~0.31 V at pH = 4 and 7; the potential characterized the oxidation of catechol groups to the corresponding quinones. Overall, both cyclic voltammetry measurement and UV-Vis spectroscopy indicated that high proportions of hydrophobic monomers in the copolyampholyte provided resistance towards catechol oxidation as a consequence of shielding effect of hydrophobic and hydrophilic units. At pH of 4, a detachment force of the coated coacervate from mica surface was ~17.0 mJ m^{-2}. At pH of 7, the bonding strength was 32.9 mJ m^{-2} and the adhesion occurred without oxidative cross-linking.

In their second work[55], they translated the *Mfp* chemical architecture to the design of zwitterionic one-component adhesive systems with

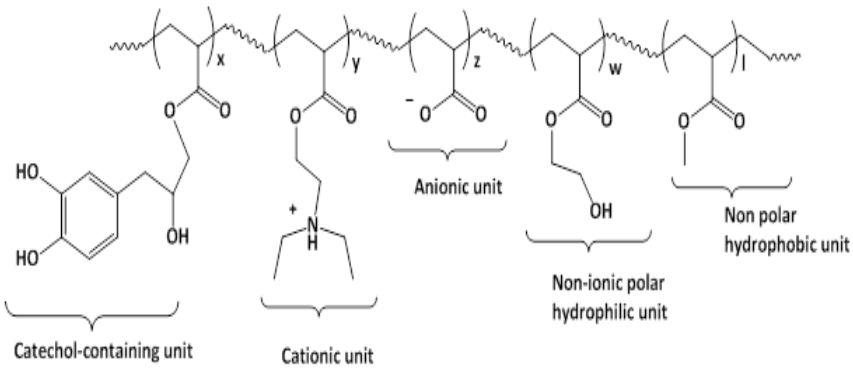

Fig. 2. Mfp-3s-mimicking copolyampholyte

low molecular weights (<500 Da), and endowed with catechol units, quaternary ammoniums as positive charges, phosphates as negative charges, and alkyl groups as nonpolar segments (equation 5). A strong wet adhesion of these zwitterionic adhesives to mica surface upon oxidation-ensued crosslinking was noticed (~50 mJ m^{-2}). The wet cohesion energy of the uncrosslinked counterparts, however, was found to be alkyl-depended in a non-systematic way: 19.2 mJ m^{-2} (R = *n*-butyl), 9.6 mJ m^{-2} (R = *n*-hexyl),

2.5 mJ m^{-2} (R = *n*-octyl), 10.1 mJ m^{-2} (R = *n*-decyl).

In their third work[56], they conceived an adhesive inspired from cement proteins of sandcastle worms which consist of DOPA-containing

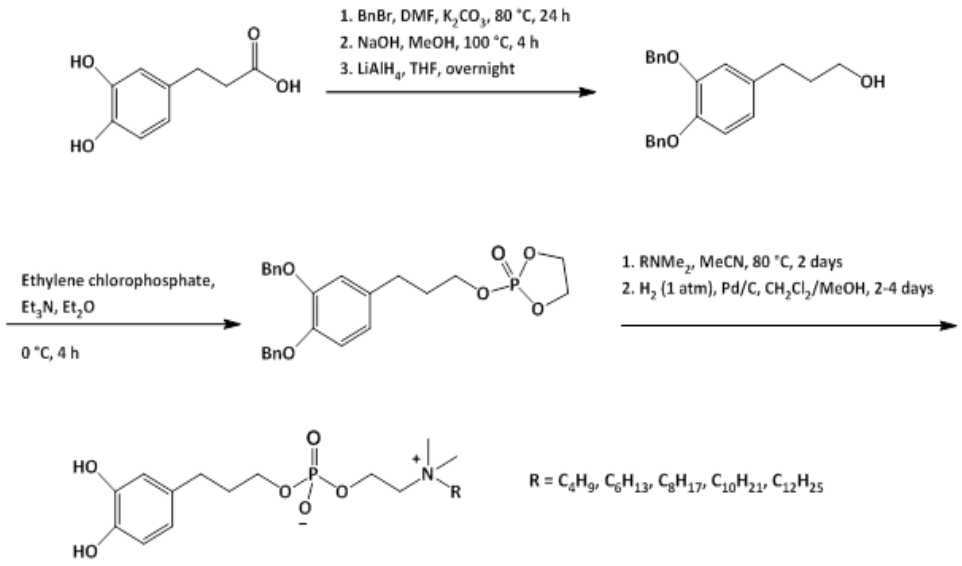

(5)

polyelectrolytes (polyanionic and polycationic proteins). The authors made a catechol-functionalized poly(acrylic acid) (Fig. 3A) and a quaternized chitosan paired with bis(trifluoromethane-sulfonyl)imide (Fig. 3B). When the mixture of the two biomimetic polyelectrolytes in DMSO was spread onto an underwater glass plate, an adhesion took place within 25 s. The set adhesive showed a resistance to a water jet of 30 bars and withstood to boiling water for 1 hour. The adhesive mechanism was reasoned in terms of a polyelectrolyte complexation that resulted from water-DMSO solvent exchange. Wet adhesion of this system was measured to be $\geq$ 2 J m^{-2} and was successful for other substrata such as polymers, metals, glasses, mussel shell, stone, leaf and wood.

Waite's school[57] went deeper in their investigation by excavating into the mechanistic

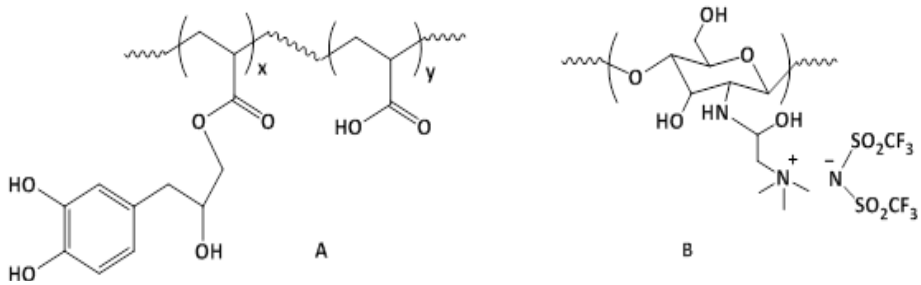

Fig. 3. Sandcastle worm proteins-mimicking polyelectrolytes

bioadhesion of *Mfp-5*. This work has shed light into the electrostatic effects and the peptide chain length on the bridge adhesion. A sound demonstration of the adhesion of three synthesized DOPA-bearing peptides with a number of residues lower (15-17 residues) than that of *Mfp-5* (75 residues) was undertaken. At pH 3, the strongest adhesion force to mica surfaces of the short DOPA-containing peptides was 4 mN m^{-1} (work of adhesion of 0.64 mJ m^{-2}), that is, more than an order of magnitude less than *Mfp-5*. At higher pH (7.5), the adhesion work dropped up to 80% as a result of the auto-oxidation of DOPA units, the loss of hydrogen-bonding making of DOPA with a mica surface, and the electrostatic interactions by positive amino acid residues. At pH3, the DOPA-bearing peptide with a number of residues

of 30 showed an adhesion force between two mica surfaces of ~6 mN m^{-1} (adhesion work =~1 mJ m^{-2}).

The film from the DOPA-containing peptide with a number of residues of 17 formed between a mica surface and a gold one had an adhesion work of ~3 mJ m^{-2}, an adhesion stronger than that between of two mica surfaces, hinting at the effect of substrate nature on bridging adhesion of the mussel-inspired peptides.

Melt polycondensation of 1,8-octanediol, PEO, citric acid, and dopamine led to adhesive materials[58]. Only adhesives with [1,8-octanediol]/[PEO]/[citric acid]/[dopamine] molar ratios of 0.3:0.7:1.1:0.3 and 0.3:0.7:1.1:0.5 were water-soluble. Their mechanical parameters were, respectively: 1.03 and 1.16 MPa (tensile strength), 2.71 and 2.86 MPa (Young's modulus), and 120.7 and 105.3% (elongation at break). The adhesion strength of the latter adhesive on porcine skin was found to be 33.7 kPa; that of α-cyanoacrylate glue was 247.6 kPa. The as-made adhesives were not highly toxic to L929 fibroblast cells as their cell viability was about 80-90%.

In a bid to improve the interfacial adhesion, mussel-inspired polydopamine was exploited in the dental resin coating, involving a light-curable glycidyl methacrylate (Bis-GMA)/triethylene glycol dimethacrylate (TEGDMA) system[59]. Towards this objective, fiber glass was coated with PDA and PMMA separately and with PMMA/PDA. The prepreg prepared from PMMA/PDA/Glassfiber and Bis-GMA/TEGDMA system was flexible, transparent, and homogeneous. The flexural strengths and moduli of the light-cured pure Bis-GMA/TEGDMA resin, Bis-GMA/TEGDMA/Glassfiber composite, Bis-GMA/TEGDMA/PMMA/Glassfiber composite, Bis-GMA/TEGDMA/PDA/Glassfiber composite, Bis-GMA/TEGDMA/PMMA/PDA/Glassfiber composite, were 113.7 and 1316.8 MPa, 900 MPa and 28 GPa, ~950 MPa and ~30 GPa, ~970 MPa and ~31 GPa, ~1000 MPa and ~32 GPa, respectively. The interfacial adhesion, taken from pull-out test, was quantified in terms of increase in the maximum failure load: 10.2% increase with Bis-GMA/TEGDMA/PDA/Glassfiber composite, 19.7% increase with Bis-GMA/TEGDMA/PMMA/Glassfiber composite, and 43.3% increase with Bis-GMA/TEGDMA/PMMA/PDA/Glassfiber composite. In view of enhancing the interfacial and interlaminar shear strengths (IFSS and ILSS) of fiber-reinforced composites, Lee and his co-workers[60] coated carbon and glass fibers (CF and GF) with polydopamine (PDA) and polynorepinephrine (PNE) in Tris solution (pH = 8.5, Tris: tris(hydroxymethyl)aminomethane) of DA or NE. The water contact angles of uncoated CF, uncoated GF, PDA-CF, PDA-GF, PNE-CF, and PNE-GF were 76.2°, 72.3°, 65.1°, 64.5°, 61.9°, and 60.2°, respectively. Their respective diiodomethane contact angles were 75.9°, 55.4°, 73.8°, 47.6°, 74.1°, and 46.7°. And, their surface free energies were 31.3, 40.2, 38.9, 47.1, 41.1, and 49.8 nM M-1. An increase in IFSS of 37, 28.9, 26.8, and 18.3% was observed for PDA-CF/epoxy resin, PNE-CF/epoxy resin, PDA-GF/epoxy resin, and PNE-GF/epoxy resin, respectively, compared to uncoated CF and GF. As to ILSS, an enhancement of 12.9, 10.5, 9.4, and 7.0%, respectively, was gained.

How good are the anti-fouling properties of mussel-inspired polymeric coatings?

A number of anti-fouling biomaterials have been conceived in tune with the nature inspiration[61]. Catecholamine-containing copolymers (Fig. 4) with antifouling properties have been synthesized by free radical copolymerization of appropriate hydrophilic comonomers[62]. The involved monomers were dopamine methacrylamide (DAMAAm), poly(ethylene glycol) methyl ether methacrylate (PEGMEMA), *N*-hydroxyethyl acrylamide (HEAAm), N-(3-aminopropyl)methacrylamide hydrochloride (APMAAm). PEGMEMA in the copolymer would provide protein repellency, whereas DAMAAm its adhesiveness. The average molecular weights Mns of the copolymers and their polydispersity indexes Ips were 28 700-62 300 g mol^{-1} and 1.26-3.10. P(PEGMEMA-co-DAMAAm) and P(HEAAm-co-DAMAAm) were able to coat the surface of stainless steel that was previously treated with piranha solution (mixture of conc. H_2SO_4 and H_2O_2), provoking the formation of hydroxyl groups on the surface; the adhesion was thought to occur via coordination interaction of the catechol groups with the surface. The coating by P(PEGMEMA-co-DAMAAm-co-APAM) and P(HEAAm-co-DAMAAm-co-APMAAm) was induced, however, by a self-crosslinking under a pH of 10. XPS analysis and static water contact angle (θ_w) measurement

confirmed the success of the coating; θ_w decreased from 78° for bare stainless steel to 51, 40, 47, and 39° for P(HEAAm-co-DAMAAm), (PEGMEMA-co-DAMAAm), P(HEAAm-co-DAMAAm-co-APMAAm) and P(PEGMEMA-co-DAMAAm-co-APMAAm), respectively. The thicknesses of their corresponding coatings on quartz surfaces were 5.5, 7.0, 33.3, and 27.4 nm, indicating greater coatings of the self-crosslinked copolymers. The coatings of the latter ones were more stable than the former ones when treated with artificial seawater at 13 cm s^{-1} for 14 days. A qualitative fluorescence microscopy analysis revealed that the adhesion of live *Pseudomonas sp*. cells was greater in the case of uncoated stainless steel surface, while there were reduced numbers of viable cells in the case of coated ones, hinting at the antifouling capacity of the coatings. Quantitatively, the relative adhered numbers of cells onto the coated surfaces were 33.8, 13.4, 19.6, and 9.2% for P(HEAAm-co-DAMAAm), (PEGMEMA-co-DAMAAm), P(HEAAm-co-DAMAAm-co-APMAAm) and P(PEGMEMA-co-DAMAAm-co-APMAAm), respectively, with respect to that of virgin stainless steel surface. This indicates that PEG-based coatings were more efficient in terms of bacterial antifouling. However, the HEAAm-based coatings performed better in the antifouling for Amphora coffeaeformis cells. The latter two coatings showed to be more effective in reducing the adhesion of barnacle cyprids than the former two ones. RAFT technique was employed by Detrembleur's team[63] to synthesize a series of block copolymers of dopamine acrylamide (DAAAm) and poly(ethylene glycol) methyl ether acrylate (PEGMEA), P(PEGMEA-b-DAAAm), and of dopamine methacrylamide (DAMAAm) and poly(ethylene glycol) methyl ether methacrylate (PEGMEMA), P(PEGMEMA-b-DAMAAm) (Fig. 4), to be evaluated for protein repellency. Molecular weights M_ns of these copolymers fluctuated between 13 000 and 42 000 g mol^{-1} and their I_ps between 1.12 and 1.25. For each copolymer, two T_gs were detected and were assigned to the two constitutive segments, respectively. The copolymers could be self-assembled into spherical micelles with average diameters of ~20 nm. By means of QCM-D measurements, the block copolymers coated to gold surface showed better BSA anti-fouling (6-47% for P(PEGMEA-b-DAAAm), 2-8% for P(PEGMEMA-b-DAMAAm)) than the uncoated one (100%). Also, the extent of adsorbed BSA protein was proportional to the content of the catechol block.

Kang's school[64] designed catechol-PEG conjugates (Cat-PEG) through a step-growth polymerization of PEG diglycidyl ether with dopamine (equation 6). Cat-PEG was transformed into a zwitterionic polymer by alkylsulfonation, giving the sulfobetaine system SBet-Cat-PEG. The adhesion of the two catechol-functionalized PEGs to stainless steel (SS), silicon wafer (Si), and titanium

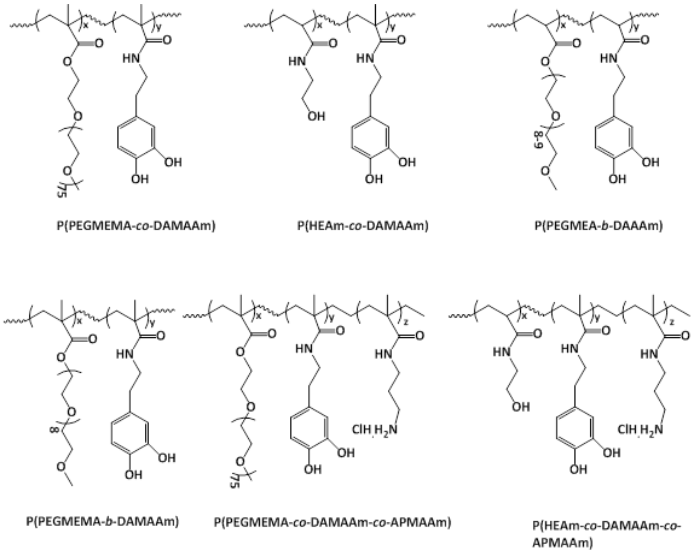

Fig. 4. Copolymers of dopamine methacrylamide (DAMAAm), poly(ethylene glycol) methyl ether acrylate (PEGMEA), poly(ethylene glycol) methyl ether methacrylate (PEGMEMA), N-hydroxyethyl acrylamide (HEAAm), N-(3-aminopropyl) methacrylamide hydrochloride (APMAAm)

(Ti) surfaces was confirmed by XPS analysis and also by the static water contact angle (θ_w) lowering, from hydrophobic surfaces (θ_w = 72.7° (SS), 86.1° (Si) and 60.4° (Ti)) to hydrophilic ones (θ_w = ~ 30-55 °). The surface ζ-potentials of these polymeric coatings, Cat-PEG and SBet-Cat-PEG, were negative and ranged from -3.4 to -50.4 and -24.6 to -53.8 mV, respectively. By means of fluorescence technique, the antifouling properties of the Cat-PEG and SBet-Cat-PEG coatings on SS against the protein fluorescein *iso*thiocyanate labeled bovine serum albumin (FITC-BSA) were demonstrated. Also, the coatings potentially inhibited the adsorption of bovine plasma fibrinogen (FBG), bacteria *(Pseudomonas sp., E. coli*), and algae *(Amphora coffeaeformis)*. This adsorption inhibition of protein, FBG, bacteria, and algae was reasoned in terms of repulsive forces that arose from the formation of a hydration layer on the hydrophilic surface, particularly for the zwitterionic sulfobetaine-containing SBet-Cat-PEG coating. These catechol-based coatings showed cytotoxicity towards 3T3 fibroblasts. Recently, the same investigators[65] reported the effectiveness of tannic-functionalized agarose in the anti-biofouling of bovine serum albumin (BSA) and Escherichia coli and 3T3 fibroblasts on various substrata such as stainless steel, titanium foils, and silicon wafer; to recall, tannic acid is a macromolecule containing gallol moieties.

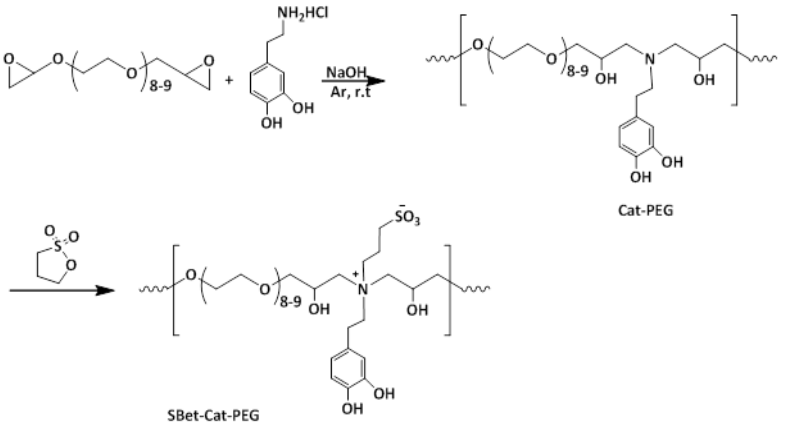

(6)

Ding *et al.,*[66] patented their work on the antifouling and antimicrobial properties of dopamine modified polycarbonates which contained PEG segments and cationic side chains consisted of ammonium or phosphonium groups or both (Fig. 5). The PEG segments provided the antifouling property of the catechol-containing polycarbonate and the cationic side chain provided its antibacterial activity. Indeed, the as-modified polycarbonates exhibited resistance to *S. aureus and S. epidermidis*.

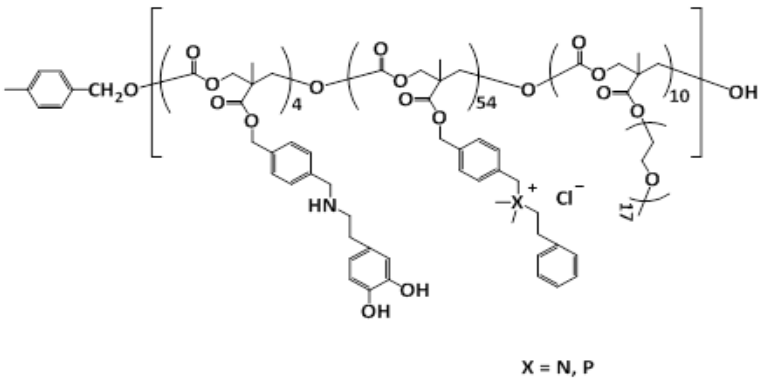

Fig. 5. Dopamine-functionalized polycarbonates

Poly(*N*-[3-(dimethylamino)propyl] methacrylamide), P(DMAPMAAm), and poly(*N*-dopamine methacrylamide-co-*N*-[3-(dimethylamino) propyl] methacrylamide), P(DMAAm-co-DMAPMAAm) (Fig. 6) were screened for their capacity to bind bacteria[67]. The incubation of the *S. aureus, V. harveyi*, *E. coli* and *P. aeruginosa* in PBS solutions of these polymers for one hour led to a substantial clustering level. Such clustering was due to the the interactions between these polyelectrolytes with the negatively charged cell wall of bacteria strains. The extents of aggregations and their sizes were pH- and bacterium concentration-dependent, and each polymer acted differently towards the strains. Besides the positive role of catechol, the interplay of charge and hydrophobicity on the clustering ability of bacteria was demonstrated.

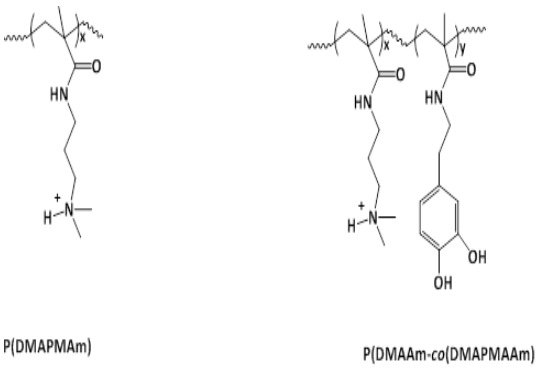

Fig. 6. Poly(N-[3-(dimethylamino)propyl] methacrylamide), P(DMAPMAAm), and poly(N-dopamine methacrylamide-co-N-[3-(dimethylamino)propyl] methacrylamide), P(DMAm-co-DMAPMAAm)

Poly(sulfobetaine methacrylate)-catechol conjugates (Fig. 7) served as coatings for hydrophobic electrospun poly(L-lactic) acid (PLLA) films[68]. The coating polymers were prepared through an ATRP technique (atom transfer radical polymerization), with molecular weights M_ns of 12 200, 23 300, and 39 500 g mol^{-1} and polydispersity indexes I_ps of 1.29, 1.34, and 1.24; the ATRP initiator was made by reacting t-butyldimethylsilyl-protected dopamine. HCl with bromoisobutyryl bromide. The coating of electrospun PLLA films with the conjugates provided a hydrophobicity lowering as suggested by the measured water contact angle θ_w. The latter angle decreased from 121° for uncoated PLLA film to 92, 22 and 0.0° when coated with poly(sulfobetaine methacrylate)-catechol conjugates with M_ns of 39 500, 23 300, and 12 200 g mol^{-1}, respectively. PLLA films coated with poly(sulfobetaine methacrylate)-catechol conjugates showed strong resistance to BSA adsorption, and this adsorption decreased with decreasing molecular weight of the coating polymer. The adsorbed extent of FITC-BSA on uncoated PLLA film was 37.5 mg m^{-2}, and those on coated ones were 1.95, 1.43, and 0.06 mg m^{-2}, respectively.

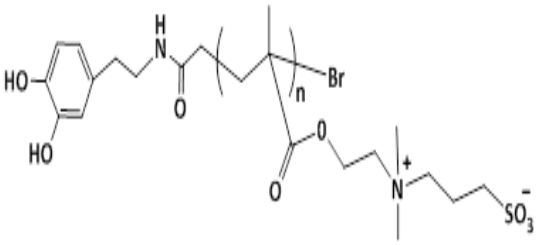

Fig. 7. Poly(sulfobetaine methacrylate)-catechol conjugate

Liu and Huang[69] functionalized polydopamine-coated substrates with sulfobetaine acrylamide, sulfobetaine methacrylate, and poly(ethylene glycol)methacrylate through β-amino carbonyl linkages by means of aza-Michael addition with α,β-unsaturated ketones, ending up with antifouling coatings (equation 7). The adherends (TiO_2, Au, SiO_2, Nitinol alloy, PDMS, and PS) were first coated with polydopamine (PDA), which resulted from an oxidative self-polymerization of dopamine in the Tris buffer at pH 8.5, followed by the different functionalizations. The hydrophobicity of the substrates decreased upon coating with PDA and with their subsequent functionalizations as revealed by the lowering of the measured static water contact angles, θ_w. For example, θ_w dropped from 63.5° for bare TiO_2 to ~22° when coated with PDA and to ~5-8° upon functionalization with sulfobetaine acrylamide; this superhydrophilicity was ascribed to the zwitterionic sulfobetaine groups which strongly interacted with water molecules via ionic solvation. Functionalization of PDA-coated TiO_2 with poly(ethylene glycol)methacrylate, having a large hydrodynamic radius, induced θ_w values of 38-43°. The viabilities of NIH-3T3 fibroblast cells to functionalized PDA-coated TiO_2 were in the range of 85%. As to bio-antifouling, the coating of PDA-TiO_2 with sulfobetaine acrylamide exhibited the best performance in fouling resistance towards *P. aeruginosa, E. coli, and S. epidermidis*, and was quantified relatively to the bare TiO_2 as 93, 94.2, and 98%, respectively.

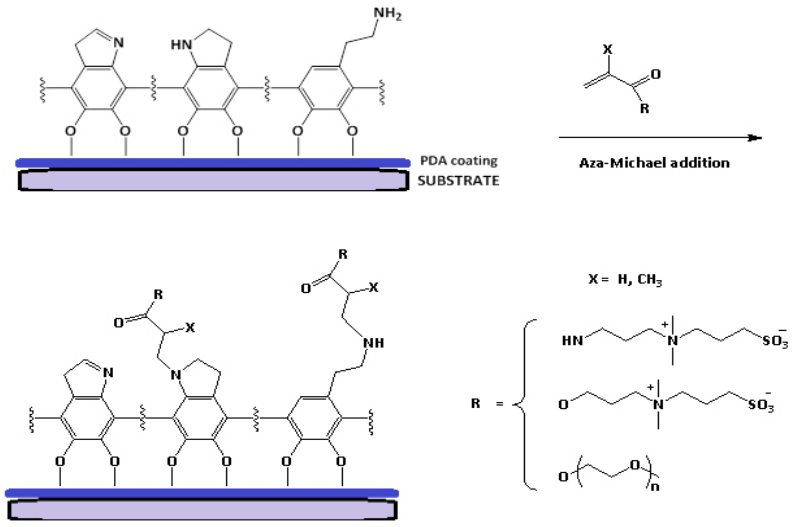

(7)

Gong and his team[70] anchored catechol (Cat) and phosphorylcholine (PC) units at the ends of an eight-arm PEG to make up anti-biofouling membranes. The thus-functionalized PEGs (Cat-PC-PEGs) were highly water-soluble. Their wet adhesiveness to gold chips were catechol content-dependent; the higher the catechol content, the greater the adhesion. Yet, the wet adhesion rate was found to be slow, a fact that could be improved if the adherend was precoated with polydopamine; indeed, the amount of adhered materials rose to ~80-215% and polydopamine favored a better adhesion of PEG with a phosphorylcholine content, a more hydrophilic polymer. The hydrophobicity of the gold chips decreased when coated with polydopamine, followed by treatment with Cat-PC-PEGs as the static water contact angle dropped from 101° (untreated surface) to 67.3° (polydopamine-coated surface) and to 43-48° (polydopamine-coated surface treated with Cat-PC-PEGs). Coating of gold surface with polydopamine resulted in reduced protein adsorption (bovine serum albumin BSA, and fibrinogen Fg) and more significantly (up to 98 and 75%, respectively) when polydopamine-coated gold was treated with Cat-PC-PEGs. Also, the latter treatment promoted anti-biofouling of platelet, L929 cell, and bacteria *(E. coli, P. aeruginosa, S. aureus)* to about 90, 99, and 85%, respectively. As reported by the same school[71], the coatings of PDA on gold chips (surface plasmon resonance sensor chips) were subjected to surface modification by treatment with $NaIO_4$ or $FeCl_3$, thermal treatment at ambient atmosphere (at 130 °C), and reaction with copolymer of methacryloxoethyl phosphorylcholine and p-nitrophenoxycarbonyloxyethyl methacrylate. The resulting modified PDA/SPR systems were evaluated for their anti-biofouling performance. The PDA coating thickness (~0.5-3.5 nm) was pH-depended; the more basic the solution, the thicker the coating. Adsorption of proteins (BSA and Fg) grew linearly with the deposited amount of bare PDA to which the coating thickness and the generated surface roughness were related. The molecular structure of PDA coating and the extant chemical functionalities (hydroxyls, amines, aromatics) would have had an effect on such adsorption. The mentioned modifications would have lessened the reactivity of such functional groups with proteins via Michael addition reaction or Schiff base reaction, and therefore reduced their biofouling. About 32-54% of BSA and Fg adsorption were suppressed by Fe(III)-chelated, $NaIO_4$-oxidized, or heated PDA coating. An excellent anti-biofouling was observed with the modification of PDA with the copolymer; the coating showed a resistance to 98.6% of BSA and 95.9% of Fg. Also, this copolymer-modified PDA coating exhibited 99% efficiency of anti-biofouling for platelet, L929 fibroblast and bacteria *(E. coli and S. aureus)*. The same school[72] recently developed a polyethersulfone ultrafiltration membrane (PES-UFM) coated with a material that consisted of polydopamine (PDA) and cell membrane antifouling phosphorylcholine (PC). A copolymer containing PC and dopamine units (Fig. 8) served as a coating for PES-UFM and

PDA-precoated polyethersulfone ultrafiltration membrane (PES-UFM/PDA). The water contact angle of PES-UFM/PDA membrane decreased from ~70° to 45-50° upon coating with the copolymer, indicating a hydrophilicity enhancement of the membrane. The BSA adsorption onto the modified PES-UFM/PDA decreased by 97% compared to 75% for untreated PES-UFM and PES-UFM/PDA.

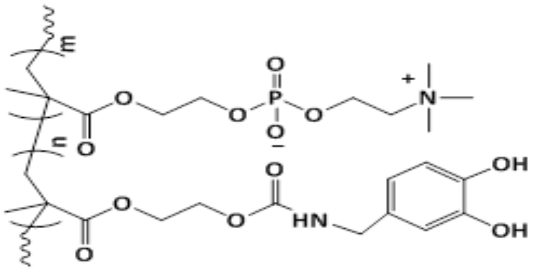

Fig. 8. A copolymer containing phosphorylcholine and dopamine units

Zhao's team[73] constructed a polyethersulfone (PES)-based ultrafiltration membrane by coating with catechol-conjugated O-carboxymethyl chitosan and polyurethane. The coatings were further loaded with Ag nanoparticles to provide to the membrane with antibacterial and antifouling properties. The as-made membrane showed an anti-fouling ability towards BSA, as a significant drop of BSA adsorption was noticed compared to that by pristine PES membrane. Also, the good antibacterial property of the constructed membrane was demonstrated against *E. coli and S. aureus.*

Waite and his collaborators[74] engineered a material with poly(ethylene oxide) loops conjugated with catechol units at the two end blocks (equation 8), mimicking the chemical structure of the mussel adhesive protein, *Mfp-2*. As shown, the silyl-protected catecholic monomer functionalized the triblock copolymers poly(EO-co-AGE)-b-PEO-b-poly(EO-co-AGE) via a thiol-ene reaction using 2,2-dimethoxy-2-phenylacetophenone (DMPA) as a photochemical initiator. At pH3, the thus-made triblock polymers showed good antifouling properties against MC-3T3, mammalian cells, and *Porphyra suborbiculata*, a marine red alga; at this pH, a silyl group deprotection occurred, generating free catechol moiety. At this pH, the lubricating effect of the catechol-functionalized ABA triblock copolymer between two mica surfaces was demonstrated and was imputed to the loop conformation of PEO segments; the measured friction coefficient, μ, varied between 0.002 and 0.004.

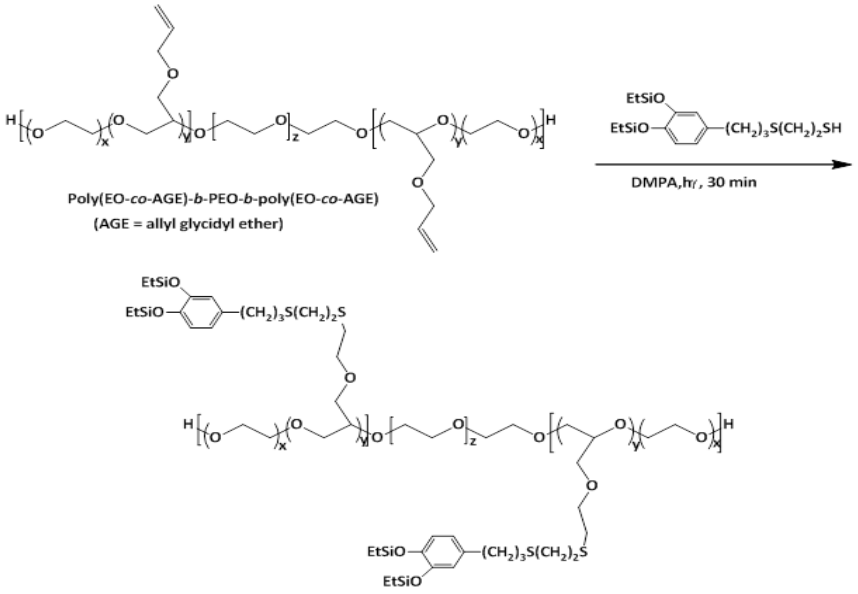

(8)

Catechol-functionalized ABA triblock copolymer, poly[(N,Ndimethylacrylamide)-co-(N-3,4-dihydroxy phenethylacrylamide)]-b-poly (ethyleneglycol)-b-poly[(N,N-dimethylacrylamide)-co-(N-3,4-dihydroxyphenethylacrylamide)], and catechol-functionalized AB diblock copolymer

were prepared via RAFT polymerization[75]. The dopamine-modified polyacrylamide ensured the adhesive property of the anti-fouling material and the poly(ethyleneglycol) its loop segment. By means of quartz crystal microbalance with dissipation (QCM-D), the anti-biofouling of the loop-coated material (ABA) on silica substrate was found to be 94%, whereas that of the brush-coated one (AB) was lower (86%). Before rinsing, the amounts of BSA protein adsorbed were: 3775.2 ng cm^{-2} for bare silica surface, 1980.0 ng cm^{-2} for brush-coated silica surface, and 567.6 ng cm^{-2} for brush-coated silica surface. After rinsing with PBS, they were 937.2, 277.2, and 31.7 ng cm^{-2}, respectively.

Hollow capsules made by reacting an 8-arm PEG/catechol conjugate (Fig. 9) with $FeCl_3 \bullet 6H_2O$ solution were reported to be low-fouling and pH-degradable items[76]. The 8-arm PEG/catechol conjugate was prepared by reaction of 8-arm-poly(ethylene glycol) succinimidyl succinate with dopamine in the presence of triethylamine at room temperature for 12 h., A color shift from colorless, green, blue, purple to red when the pH was increased from 3 to 11 for the reaction between PEG/catechol conjugate and Fe(III) solution, which was assigned to the transition of coordination complexes from mono- to bis- to tris-catechol complexes; treatment with Fe(III) promoted the crosslinking[6] and, henceforth, the formation of capsules. The capsules readily collapsed upon lowering the pH.

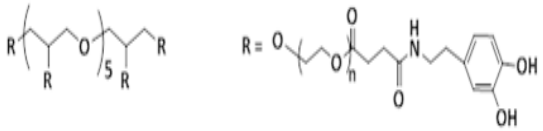

Fig. 9. Eight-arm PEG/catechol conjugates

In view of improving the anti-biofouling property of silicone, silicone rubber surface was coated with dopamine-terminated PEG (DA-PEG) and dopamine-functionalized hyaluronic acid (DA-HA) in Tris-HCl solution (pH = 8.5) and at different immersion times and temperatures[77]. The water contact angle of parent silicone rubber (88°) decreased to as low as 50° upon DA-HA and DA-PEG coatings; the higher amount of the coating, the lower the decrease. The coated silicone rubber exhibited a significant anti-fouling for BSA and Fg (fibrinogen) compared to the higher adsorption by the unmodified rubber; this finding was attributed to the enhanced hydrophilicity of the modified silicone rubber. Also, the population of adsorbed platelets on the modified was lower than that on unmodified silicone, and decreased with a number of coated layers. According to the results of APTT assay, DA-PEG and HA multilayer coatings showed an improved anti-coagulant property and blood compatibility. Such coatings also revealed a solidity against cells such as NIH3T3 fibroblasts, suggesting their non-cytotoxicity.

Xu and his research team[78] investigated the surface hydrophilization and antifouling property of polypropylene microfiltration membrane (PP-MFM) by immobilizing TiO_2 nanoparticles TiONPs (diameter = 10-50 nm) via polydopamine/polyethyleneimine (PDA/PEI) coating; PEI was claimed to reduce the PDA aggregation and induce its deposition. To realize such PP-MFM modification, the PDA/PEI-coated PP-MFM was immersed into titanium (IV) bis-(ammonium lactate) dihydroxide/$NH_3.H_2O$ solution for a given time at room temperature. The TiONPs-modified PP-MFM was stable in alkaline solutions and less stable in acidic solutions, particularly unstable in solutions with pH < 4. In strong acidic media, the coordination interaction between TiONPs and PEI molecules is weakened due to the protonation of the amino groups in PEI. Moreover, PDA is known to be unstable in strong acid solution, causing the loss of TiONPs. The water contact angle of the TiONPs-modified PP-MFM was measured to be 0°, suggesting its superhydrophylicity. The water flux of the pristine PP-MFM, PDA/PEI-coated PP-MFM, and TiONPs-modified PP-MFM was 605, 4400, and 5720 L m^{-2} h^{-1}, respectively. The antifouling property of the TiONPs-modified PP-MFM was evaluated by relative flux reduction (RFR) and the flux recovery ratio (FRR) for bovine serum albumin (BSA) and lysozyme (Lys). FRRBSA increased from 44% for the virgin membrane, to 70% for PDA/PEI-coated membrane, and to 82% for TiONPs-modified PP-MFM. RFRBSA decreased from 72% to 52% and to 31%, respectively. About the same trends of RFRLys and FRRLys were observed. The higher values of FRR and lower ones of RFR for BSA and Lys were strong indication that TiONPs-modified PP-MFM proved to be endowed with great an antifouling property towards proteins.

A hybrid coating involving PDA and poly(sulfobetaine methacrylate) (PSBMA), a

zwitterionic polymer, on polypropylene microfiltration membrane (PPMM) was rapidly mounted using $CuSO_4/H_2O_2$-trigger for the PDA formation[79]. The PDA/PSBMA-coated PPMS exhibited antifouling property against bacteria such as *E. coli*, the quantity of its bacterial adhesion being estimated as only 10% of that of bare PPMS. Overall, the long-term antifouling performance of the as-coated PPMS was mainly due to the outstanding stability and durability of the structure of $CuSO_4/H_2O_2$-triggered PDA/PSBMA; this $CuSO_4/H_2O_2$ method afforded more covalent bounds and crosslinkings than in air oxidation.

Xue and his collaborators[80] examined the under seawater superoleophobicity of PDA-coated conventional PVDF membrane. To accomplish this, the pristine membrane was first treated with PEG in the presence of triethylphosphate, followed by immersion into Tris solution (pH = 8.5) of dopamine. The average pore size of the as-modified PVDF membrane decreased with increasing immersion time: 42.3 nm (t = 0 h), 39.7 nm (t = 6 h), 36.6 nm (t = 12 h), and 28.2 nm (t = 24 h). The antifouling ability against proteins was demonstrated by experimenting with bovine serum albumin (BSA); indeed, the relative flux reduction RFRBSA and the flux recovery ratio FRRBSA were: RFRBSA = 14.5% (t = 0 h), 12.6% (t = 24 h); FRRBSA = 61.8% (t = 0 h) and 96.1% (t = 24 h).

How well and useful are the nanoparticles designed with mussel-inspired polymers?

Metal oxide nanoparticles, MONPs

Nanoparticles of various inorganic compounds such as metal oxides (MONPs) and metals (MNPs) have been usually coated with organic films for various aims. The synthesis of the uniformly-sized iron oxide nanoparticles (IONPs) and the use of hydrophilic polymer modules with them have been well-documented[81]. Peculiarly, uniform IONPs have been versatile in biomedical applications including diagnostic imaging and cell tracking, particularly the polydopamine-coated IONPs[82].

Catechol-terminated poly(vinyl alcohol) (Fig. 10), produced by alkaline hydrolysis of poly(vinyl acetate) (PVAc) that was achieved by RAFT polymerization of vinyl acetate, was anchored onto superparamagnetic iron oxide nanoparticles (IONPs)[83]. PVAc was obtained with an average molecular weight of 2.3 kDa and a polydispersity of 1.2. both single and clustered nanoparticles were formed upon mixing oleic acid-coated iron oxide particles with catechol-terminated poly(vinyl alcohol) in water through ligand exchange process. The thus made forms of nanoparticles remained stable in water, and could be easily separated from each other.

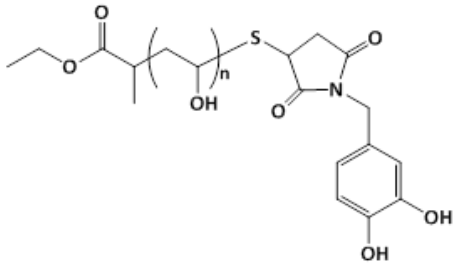

Fig. 10. Catechol-terminated poly(vinyl alcohol)

A work on anticancer drug release from smart magnetic nanoplatforms involving IONPs, poly(2~hydroxyethyl methacrylate~co~dopamine methacrylamide) (P(HEMA~co~DAMAAm)), or electrospun nanofibers of poly(methyl methacrylate-co-dopamine methacrylamide) (P(MMA-co-DAMAAm)), and Bortezomib (BTZ), was launched by Kim and his co-workers[84,85]. A dual treatment combining hyperthermia and chemotherapy was sought for from these nanocomposites. To this end, P(HEMA~co~DAMAAm)-BTZ,P(MMA~co~DAMAAm)-BTZ, P(HEMA~co~DAMAAm)-IONPs, P(MMA~co~DAMAAm)-IONPs, P(HEMA~co~DAMAAm)-IONPs/BTZ and P(MMA~co~DAMAAm)-IONPs/BTZ were prepared and characterized. The immersion of P(MMA~co~DAMAAm) nanofibers (average diameter = 800 nm) into IONPs (average diameter < 20 nm) solution with a pH adjusted to 8.5 resulted in a color change from white to brown, indicating the catecholic-metal conjugation in the product P(MMA~co~DMA)-IONPs. The P(MMA~co~DAMAAm)-BTZ nanofibers prepared by electrospinning the solutions of P(MMA~co~DAMAAm) and BTZ were immersed into IONPs to obtain P(MMA~co~DMA)-BTZ/IONPs. However, the drug bound magnetic p(HEMA~co~DAMAAm)-IONPs/BTZ was prepared by mixing first the BTZ to P(HEMA~co~DAMAAm), allowing complexation of catechol units of the copolymer to boronic acid units of BTZ, followed by addition of oleic acid-treated IONPs to ensure a ligand exchange between oleic acid and the remaining

catechol units. P(MMA~co~DAMAAm)-BTZ/IONPs and P(HEMA~co~DAMAAm)-IONPs/BTZ were pH-sensitive drugs for cancer cells. In neutral or basic pH, catecholic unit of the material and boronic acid of BTZ formed a stable boronate ester, making BTZ noncytotoxic. But in an acidic environment (a cancer environment), BTZ can be readily released, and attacked the cells. The maximum release of BTZ from these magnetic nanoparticle drugs was observed at pH = 5.0; for example, 86% of BTZ release from P(HEMA~co~DAMAAm)-IONPs/BTZ was detected at pH = 5 after an incubation of 12 h and only ~20% release was observed at physiological pH (7.4). The synergetic effect of hyperthermia and chemotherapy of the magnetic nanoplatfoms was experimentally proven.

Nanochains of magnetic IOPNs were magnetically fashioned and coated with polydopamine, which resulted in scaffold for further functionalization and conjugation[86]. Treatment of aqueous solution of PDA-IONP nanochains with $HAuCl_4$ solution led to a color change from white to dark brown first and finally to red, giving rise to gold nanocatalyst-loaded magnetic nanochains, AuNPs-loaded nanochains. UV-Vis spectrum of the latter material showed a new band at 550 nm which was assigned to a localized surface plasmon resonance of individual AuPN with an average size of AuNPs of 15 nm. AuNPs-loaded nanochains were evaluated for their catalytic activity in the reduction of 4-nitrophenol with $NaBH_4$, and the results were that a rate increase of 57% was observed, from 0.132 to 0.208 min^{-1}. The conjugation of these nanochains with PEG and DNA, via Michael addition and/or Schiff base reactions, promoted their stability in buffer solutions and cell culture media. Their conjugation with PEG changed their ζ-potential from –10.8 to –1.5 mV, and that with negatively charged DNA aptamer induced a ζ-potential of –40.2 mV. The bioconjugation with DNA is of a great interest as it permits a specific recognition of the nanochains to cancer cells.

Regioselective acylation of dihydromyricetin (equation 9), giving dihydromyricetin~3~acetate, was successful in the presence of supported enzyme made by immobilization of *Aspergillus niger* lipase (ANL) onto PDA-coated magnetic IONPs (average diameter = 10 nm)[87]. The supermagnetic behavior of IONPs and PDA-IONPS is in line with their high saturation magnetization, that is, 60.1 and 52.7 $emug^{-1}$, respectively. An optimal lipase loading of 138 mg g^{-1} was reached after 12 h of immobilization operation and at a pH of 8. The optimal conversion of the acylation of dihydromyricetin catalyzed by PDA-IONPs/ANL was greater than that catalyzed with free lipase, ~79% against ~69%. The isolation of the supported biocatalyst was easily monitored by simply applying a magnet to the reaction system. The bio-nanocatalyst could be reused up to ten times with more than 55% retention of its catalytic activity.

Zhang and his co-workers[88] functionalized

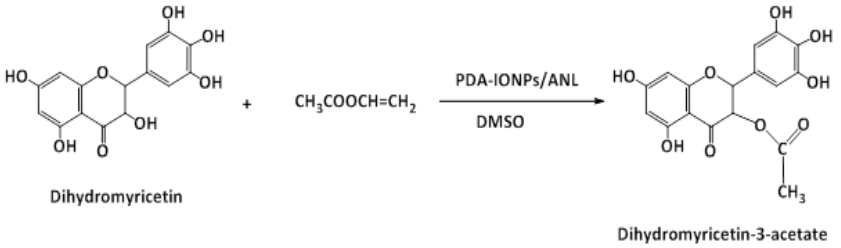

(9)

the superparamagnetic IONPs surfaces with catechol-modified copolymer of chitosan and poly(ethylene glycol) (Cat-Chit-g-PEG) (Fig. 11A) and Cat-Chit-g-PEG modified with cationic polyethyleneimine (Cat-Chit-g-PEG-g-PEI) (Fig. 11B) for gene delivery. The coatings of the nanoparticles with these polymers were accomplished by sonochemical co-precipitation of a mixture of iron chlorides (Fe(II) Fe(III)) in aqueous solution and a pH of 10.5. The ζ-potential of Cat-Chit-g-PEG/IONPs was measured to be about 5.8 3 mV and that of Cat-Chit-g-PEG-g-PEI/IONPs with 50% w/w feed ratio of Cat-Chit-g-PEG-g-PEI/Cat-Chit-g-PEG was 19.9 mV; the latter ζ was believed to be adequate enough for gene delivery. The Cat-Chit-g-PEG/IONPs and the Cat-Chit-g-PEG-g-PEI/IONPs were characterized with an average hydrodynamic size of 35 and 72 nm, respectively, and were of similar

average core diameters of ~5.2 nm. Besides, they showed high saturation magnetization of 63.1 and 51.7 emu g^{-1} Fe, respectively. The catechol functionalization of the polymer modules for IONPs enhanced the magnetic resonance imaging (MRI) contrast.

Holten-Andersen and his group[89] realized

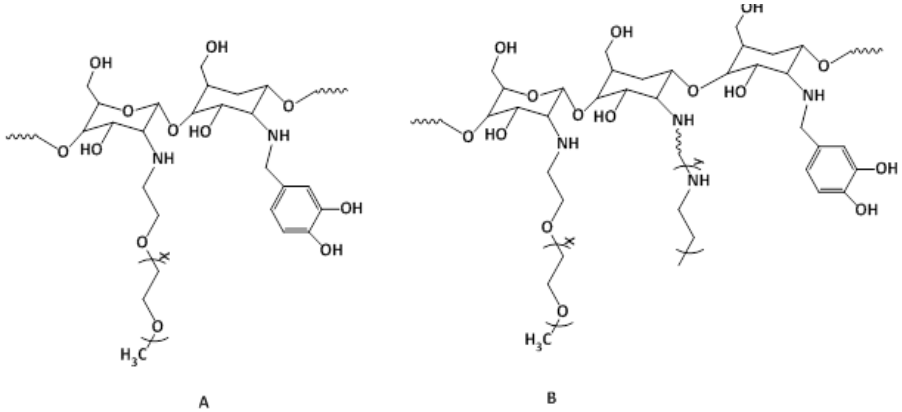

Fig. 11. A, Cat-Chit-*g*-PEG; B, Cat-Chit-*g*-PEG-*g*-PEI

hydrogels by incorporating IONPs into a catechol-functionalized PEG; the crosslinking was conceived via iron(III)-coordination bonds, stemming from the nanoparticles at concentrations higher than 52 mg mL^{-1}. Fe_3O_4 nanoparticles were first stabilized with linear monofunctionalized polyethylene glycol carboxylic acid, a hydrophilic ligand, followed by treatment with 4-arm catechol-terminated polyethylene glycol at a pH of ≈ 4-5 and at 50 °C. The as-realized hydrogels proved to be magnetically responsive due to the incorporated Fe_3O_4.

Ultrasmall superparamagnetic iron oxide Fe_3O_4 nanoparticles (USIONPs), commonly employed as contrast agents in magnetic resonance imaging (MRI), were stabilized via ligation to catechol-multidentate block copolymers (Cat-MDBCs) (Fig. 12A), providing Cat-MDBCs/USIONPs colloids with a diameter of ~20 nm[90]. The ζ-potential of Cat-MDBC/USIONP colloids was measured to be between -15 to -30 mV at pH >7 and was greater than that of Cat-MDBC, indicating that most of catechol units were actually bound to the nanoparticles. The colloids were stable at pH of 4, 7, and 9 at 37 °C as their diameter remained unchanged upon varying the pH. Also, their stability when incubated with human serum and with human IgG protein in physiological conditions (pH = 7.3, 37 °C) was proven, as neither a significant precipitation nor an aggregation occurred for different concentrations of the colloids. The cytotoxicity test of the Cat-MDBC/USIONP colloids for HEC 293T normal and HeLa cancer cells showed a viability of higher than 80%. Magnetic IONPs were also coated with catechol-multidentate chitooligosaccharide (Fig. 12B)[91]. IR analysis confirmed the formation of the Fe_3O_4-catechol coordination bond as the phenolic band at 1267 cm^{-1} disappeared. The peaks at 540, 592, and 637 cm^{-1} observed in their Raman spectrum was a strong evidence for a bidentate chelation of the metal ion by the catecholic units. The as-bound IONPs were hydrophilic, highly water-soluble, and exhibited good colloidal stability and biocompatibility; these resulting properties were due to the integrated PEG and to the catechol-multidentate ligand. The latter ligand provided them an excellent stability in highly concentrated NaCl solutions (up to 2 M) and for a wide pH range of 1-12. The cytotoxicity test of the catechol-multidentate iron oxide nanoparticles revealed their biocompatibility. Their use as contrast agents in MRI was demonstrated.

Haddleton *et al.,*[92] employed the single electron transfer living radical polymerization (SET-LRP) to prepare catechol-terminating polymeric fluorescent systems to graft magnetic IONPs, as traced in equation 10. Towards this aim, unprotected dopamine-containing molecule was used to initiate water-borne homopolymerization or block copolymerization of several acrylic monomers such as acrylamide, N-isopropylacrylamide, poly(ethylene glycol) methyl ether acrylate, 2-hydroxyethyl acrylate, glycomonomer, and Rhodamine B piperazine acrylamide. The conversions, average molecular

weights M_ns, polydisersity indexes I_ps were in the ranges of 88-100%, 3 700-22 700 g mol^{-1}, and 1.10^{-1}.135, respectively, for a reaction time ranging from 30 to 180 min. and a temperature of 0 °C, and were dependent on the [initiator]/[monomer]/[CuBr]/[Me_6TREN] ratio. The thus-formed water dispersible magnetic IONPs (diameter of ~5 to ~30 nm) were stable in aqueous environment, had good biocompatibility, and showed appreciable cell viability.

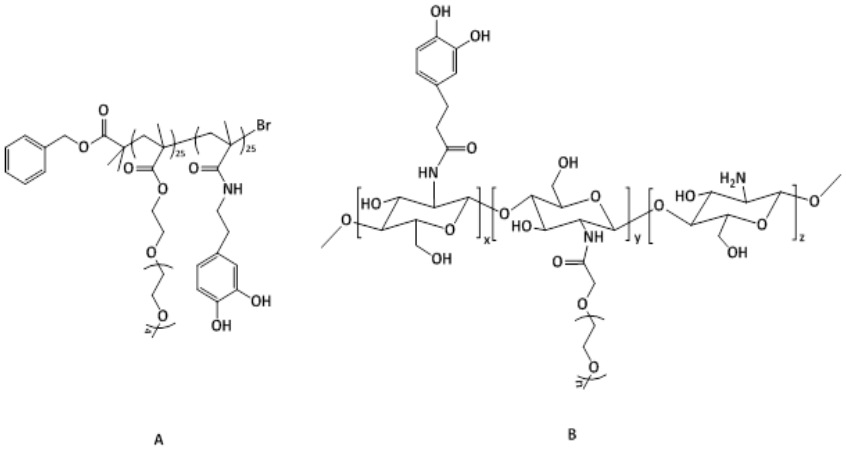

A B

Fig. 12. A, Catechol-multidentate block copolymer, Cat-MDBC; B, Catechol-multidentate chitooligosaccharide

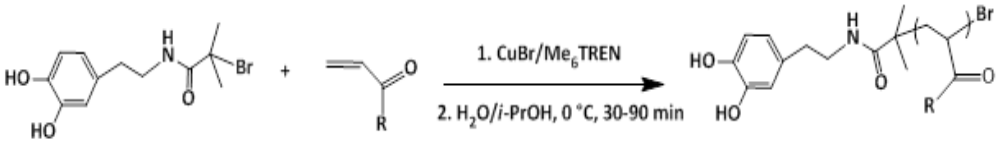

Me_6TREN = Tris[2-(dimethylamino)ethyl]amine

(10)

Chinese investigators[93] also applied SET-LRP methodology to build up core-shell magnetic iron oxide nanoparticles (Fig. 13), using polydopamine chemistry, for highly-efficient uranium enrichment. The approach involved the coating of Fe_3O_4 core with PDA film acting as shell and platform for attaching 2-bromoisobutyryl bromide, giving rise to a macro-initiator. Brushes of polyacrylonitrile (PAN) could be created by SET-LRP using this macroinitiator and Cu(0)/Me_6TREN as a catalytic/ligand system. The PAN brushes were then allowed to react with hydroxylamine to yield amidoxime-functionalized PAN, AO-PAN; the amidoxime is widely known as an efficient metal chelating ligand, particularly for uranyl ions. The average diameter and saturation magnetization of the prepared IONPs were ~100 nm and 74.3 emu g^{-1}, respectively. The adsorption of uranyl ions by the core-shell PDA-IOPN/AO-PAN was pH-dependent; the amount of adsorbed UO_2^{2+} increased with increasing pH from 3 to 5, and declined for a pH of up to 9. An optimal adsorption capacity of ~162.5 mg g^{-1} was gained at pH = 5. The kinetic parameters of the undertaken study suggested that adsorption obeyed a pseudo second-order model. Because of the superparamagnetic property of the adsorbent, the adsorbed uranyl ions could be readily desorbed by application a magnetic field, hence the enrichment of uranium.

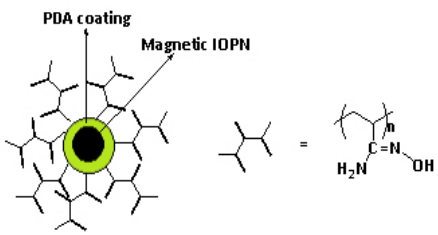

Fig. 13. The core-shell PDA-IOPN/AO-PAN

Treatment of the solution mixture of self-polymerized polydopamine particles (average diameter = 500 nm), $FeCl_2$, and $FeCl_3$ with ammonia afforded IONPs (average diameter = 50 nm) that were immobilized on PDA particles via a chelation mechanism with catecholic units[94]. The thus-generated microparticles were rendered superhydrophobic and superoelophilic upon reaction with 1H,1H,2H,2H-perfluorodecanethiol, creating a fluoroalkane layer. The superhydrophobic and superoelophilic character of the PDA-IONPs microparticles were given by its high water contact angle θ_w of 153.7°, and its hexane contact angle, θ_{hex} of 0°, respectively. These two properties and the magnetic one made the microparticles an excellent candidate in the removal of oil from aqueous media. Practically, polyurethane-base sponge bearing these superhydrophobic PDA-IONPs microparticles displayed a high hexane absorption capacity, with weight gains ranging from 1348 to 7268%.

German investigators[95] described the synthesis of catechol-containing poly(phosphoester)s (PPEs) for making hydogels therefrom and stabilizing iron oxide nanoparticles. Homopolymer and copolymer of phosphoester (Cat-PPE, Cat-coPPE)) that bear catechol units were made via acyclic diene metathesis polymerization (ADMET polymerization) of the respective monomer/comonomer in the presence of Grubbs or Hoveyda-Grubbs catalysts as illustrated in equation 11. The acetal-protected polymers were obtained with molecular weights of up to 42 000 g mol^{-1}. The acetal deprotection work-up via acidic hydrolysis was achieved without degradation or transesterification of the catechol-containing materials. The hydrogels from these catechol-containing PPEs could be formed within a few seconds either in the presence of only $NaIO_4$ at a ratio of 2:1 (polymer/oxidant) or by addition of NaOH solution first, followed by that of the oxidant. The solvent uptake of the hydrogels were 600% in water and 1 000% in ethanol. The glass transition temperature of Cat-coPPE was measured to be -59 °C, while that of its hydrogel was -51 °C. The oleic acid-treated IONPs (diameter ≈ 13.3 nm) were coated with PPEs and the Cat-coPPE showed binding affinity to the nanoparticles (*k*A = 15300 L mol^{-1}, the association constant).

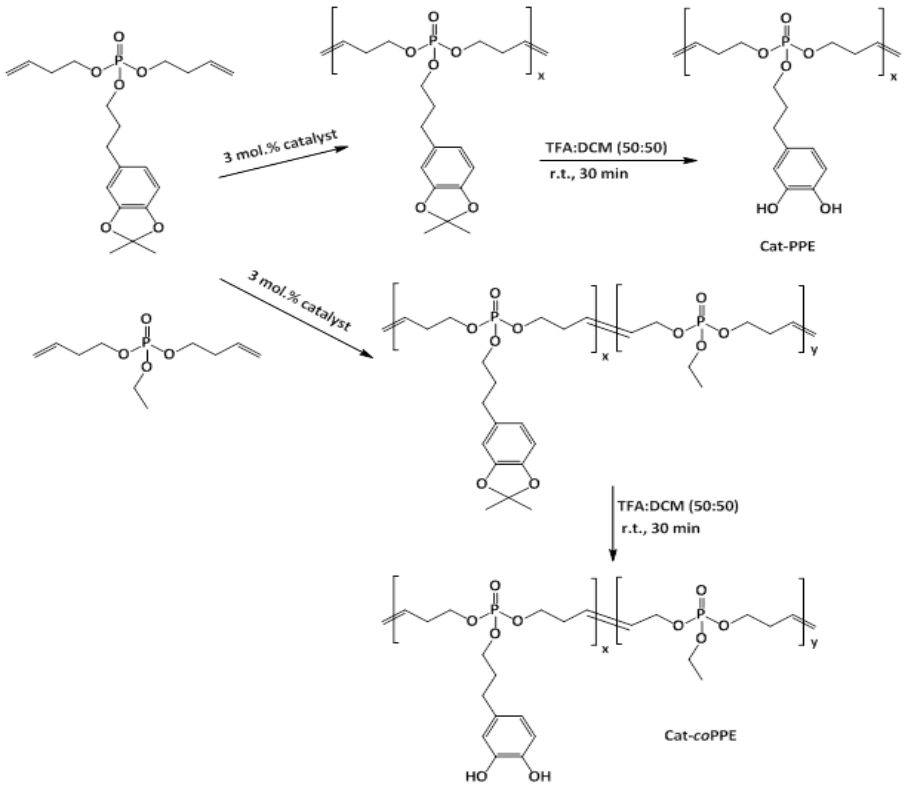

(11)

Lee and Lee[96] fashioned magnetic iron and cobalt oxides core-shell nanoparticles through the self-assembly of DOPA-containing bolaamphiphilic molecule (a bolaamphiphile is an amphiphilic molecule that has hydrophilic groups at both ends of a sufficiently long hydrocarbon chain) (Fig. 14). A mixture of this bolaamphiphile and $FeCl_3$ or $CoCl_2$ under a pH of 8 allowed the formation of the metal oxide nanoparticles after 24 h of incubation in the dark at room temperature. The sizes of cobalt and iron oxide core-shell nanoparticles were measured to be 352.3 and 402.6 nm, respectively. The magnetization property of metal oxide core-shell nanoparticles was evaluated in terms of their magnetic mass susceptibilities; they were 1.10×10^{-7} and 2.72×10^{-7} m^3 kg^{-1} for cobalt oxide and iron oxide nanoparticles, respectively, prepared from 5 mM of bolaamphiphile.

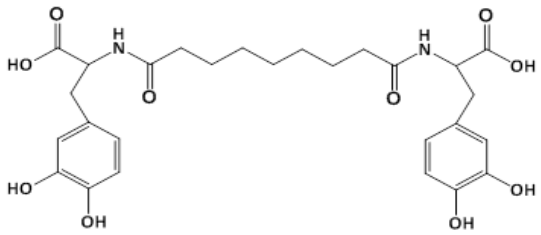

Fig. 14. DOPA-containing bolaamphiphilic molecule

Micro-scale porous structure network was constructed through the polymerization of dopamine in a mixture with hydrophilic fumed silica nanoparticles (SiONPs), using ice templates[97]. The as-prepared porous material was made superamphiphobic by treatment with 1H,1H,2H,2H-perfluorodecyltriethoxysilane, showing a super-repellency to droplets with surface tension of 73 - 23 mN/m and a static contact angle of larger than 150°.

In view of enhancing their dispersibility in water and organic media, silica nanoparticles SiONPs (average sizes of worked SiONPs were 30, 100 and 150 nm), after being coated with PDA, were subjected to functionalization with poly(N-isopropylacrylamide) (PNIPAAm)[98], a polymer of poly(ethylene glycol) methyl methacrylate (PPEGMA)[99] and a copolymer of poly(ethylene glycol) methyl methacrylate and N-(3-aminopropyl) methacrylamide, P(PEGMA-co-NAPAAm)[100] (Fig. 15). The modification of PDA-SiONPs with PNIPAAm was conducted using SET-LRP technique, and their conjugation with biocompatible polymers, PPEGMA and P(PEGMA-co-NAPAAm), was achievable through Michael addition reaction. Such undertaken functionalization has induced an improved dispersibility of the modified-SiONPs in several solvents (water, THF, DMSO), compared to the nascent SiONPs.

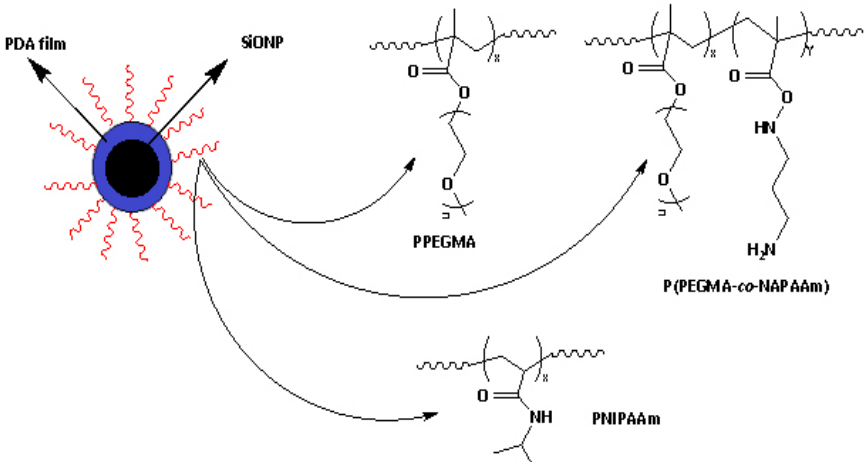

Fig. 15. PDA-SiONPs functionalized with poly(NIPAAm), poly(PEGMA) and poly(PEGMA-co-NAPAAm)

In their pursuing work on SiONPs, Wei and his group[101] provided an in situ PDA coating of the nanoparticles (diameter = 160-180 nm) upon their functionalization with dopamine-modified poly(sodium 4-vinylbenzenesulfonate-co-itaconic anhydride), (poly(SVS-co-ITA/DA)) (equation 12)

under alkaline conditions, giving rise to a core-shell structure. The PDA coating occurred through the self-polymerization of the attached DA units at pH of 8.5. Such chemical modification of SiONPs has brought up an improvement of its dispersibility in water; the ζ-potential of the as-made nanocomposite in water was measured to be 31.5 mV, hinting at its good stability in this medium. Study of the adsorption revealed that the adsorption capacity of nanocomposites towards methylene blue was nearly four-fold that of the nascent SiONPs; the equilibrium adsorption capacity of the nanocomposites was about 62.2 mg g^{-1}, and that of the raw SiONPs was approximately 16.3 mg g^{-1}. The adsorption results obeyed pseudo-first-order adsorption kinetics and Langmuir and Freundlich adsorption isotherm models.

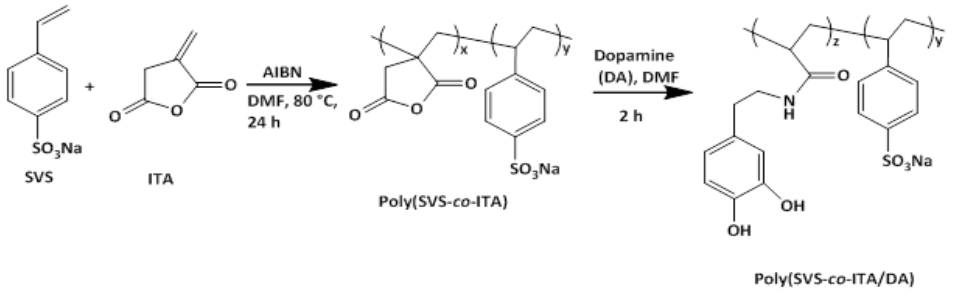

(12)

Following the same protocol as in equation 12, poly(PEGMA-IA-DA) (PEGMA = polyethylene glycol methyl ether methacrylate) was prepared and deposited on SiONPs (50-200 nm) to afford a carrier of Cisplatin (DDP, dichlorodiaminoplatinum II), a cancer therapeutic agent; the Cisplatin was ligated via the carboxylic groups offered by ring-opening of itaconic acid[102]. A DDP loading content of about 26% could be achieved when the complexation experiment was carried out in PBS (pH = 7.4) and at room temperature for 48 h. After this time, the DDP release extent was only 18 wt.% at pH of 7.4 and about 62 wt.% at pH of 5.5. By means of CCK-8 assay, the cytotoxicity test of P(PEGMA-IA-DA)-SiONPs/DDP nanocomposite against A549 cells revealed a cell viability of greater than 90%. The same research group[103] decorated PDA-coated SiONPs with poly(acrylic acid), PAA, via a combination of Michael addition reaction and mussel-inspired chemistry. The adsorption of methylene blue by PAA-PDA-SiONPs was nearly 3.5 fold that by bare SiONPs. This adsorption fitted better Langmuir isotherm model and its kinetics was found to be better described by a pseudo-second-order. The thermodynamic parameters of the adsorption at 298 K were $\Delta G° = -5.058$ kJ mol^{-1}, $\Delta H° = -12.33$ kJ mol^{-1}, and $\Delta S° = -0.02499$ kJ mol^{-1} K^{-1}, suggesting that the adsorption was spontaneous and exothermic process. Monodisperse SiONPs (diameter of 290-400 nm) coated with poly(L-DOPA), PDOPA, served as an adsorbing nanocomposite for Cu(II)[104]. The adsorption capacity of the PDOPA-SiONPs nanocomposite towards this metallic ion was about 5.5 times that of SiONPs. The Langmuir isotherm fitted the actual adsorption slightly better than the Freundlich's and the pseudo second-order equation was the more favorable kinetic model. The adsorption capacity of the nanocomposite was found to increase with temperature and with pH up 7 and to decrease at higher pHs. The thermodynamic parameters of the adsorption at 293.1 K were: $\Delta G° = -5.750$ kJ mol^{-1}, $\Delta H° = +4.993$ kJ mol^{-1}, and $\Delta S° = +0.03727$ kJ mol^{-1} K^{-1}, suggesting that the adsorption was spontaneous and endothermic process.

A layer-by-layer (LBL) assembly of nanocomposite films has been conceived by incorporating silica and titania nanoparticles (TiONPs) into catechol-functionalized polyacrylamide (Fig. 16)[105]. Catechol units from the bottom layer bound the nanoparticles through simple dipping in a dispersion of the nanoparticles. The formation of silica- and titania-polymer nanocomposites required a pH of 1-2 and 4.5, respectively, to promote hydrogen bonding. The thickness of one nanocomposite film layer could reach 15 to 20 nm. The as-fabricated catechol layer-by-layer platform of tunable Bragg stack coatings (photonic materials) showed improved stability to pH, to solvent and to ionic strength.

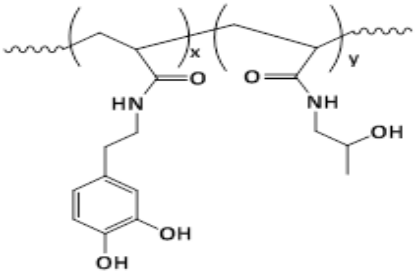

Fig. 16. Catechol-based polyacrylamide

Titania nanoparticles were bound to the PDA layer of PDA-coated polypropylene fibers to enhance the UV-resistance of the fibers[106]. The mechanical properties of the PDA-PP-TiONPs were not altered significantly after exposure to UV irradiation for 48 h., A decrease of 8.50 cN in the tensile strength was observed for polypropylene fibers after UV irradiation, while a decrease of only 1.01 cN was observed for PDA-PP-TiONPs.

TiONPs (21 nm) were chemically affixed to PDA-functionalized surface of reduced graphene oxide sheets (rGO) and were successfully valorized as a photocatalyst in the degradation of environmental pollutants such as the discarded methylene blue (MB)[107]. The photocatalytic degradation efficiency of MB was found to depend on the type of irradiation and the extent of rGO in TiONPs/PDA-rGO nanocomposite; about 100% efficiency was observed for 1 wt.% rGO under UV irradiation, and about 70% for 10 wt.% rGO under visible light. More than 93% of photocatalytic degradation efficiency could be reached after three runs with recycled TiONPs/PDA-rGO having 1 wt.% rGO and using UV source. In the same year, the same school[108] disclosed the realization of the PDMS-based microreactors, internally decorated with a catechol-containing polymer (PDA-PVP) (equation 13) which served as a platform for immobilizing TiONPs. The degree of immobilization increased with increasing DAP content in the DAP-PVP material. The degradation efficiency of MB with TiONPs/DAP-PVP/PDMS on-chip photocatalytic microreactor and using UV light was higher than 92%. This efficiency was found to be linked not only to the content of DAP but also to the flow rate of the MB solution into the microreactor. In another report, this school[109] reported the coating of polystyrene beads (PSBs) with poly(ethylene glycol)-g-poly(dimethylaminoethyl methacrylate) (PEG-g-PDMAEMA) quaternized with 2-chloro-3',4'-dihydroxyacetophenone (CDAP). The thus-modified surface of PSBs was studded with antimicrobial AgNPs, magnetic IONPs, and photo-catalyst TiONPs. The PSBs/DAP-(PEG-g-PDMAEMA)/AgNPs exhibited potential antimicrobial activity towards *E. coli and S. aureus*, compared to the non-bacterial activity of PSBs and PSBs/DAP-(PEG-g-PDMAEMA). The photocatalytic performance of PSBs/DAP-(PEG-g-PDMAEMA)/TiONPs was demonstrated for the degradation of MB under UV light; the blue color of MB faded and its absorption at λ = 663 nm decreased markedly upon irradiation for 6 h., Superparamagnetic property of PSBs/DAP-(PEG-g-PDMAEMA)/IONPs was proven by applying an external magnetic field in the presence of a permanent magnet.

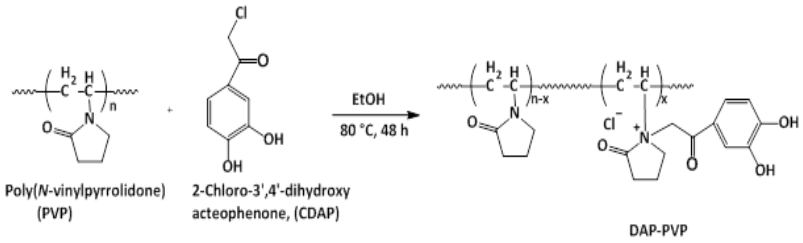

13

Nanocomposites with enhanced energy storage capacity were realized by mixing poly(vinylidene fluoride-co-hexafluoropylene) (P(VDF-HFP)) and TiO_2 nanowires functionalized with 1H,1H,2H,2H-heptadecafluorodecyl 2-amino-3-(3,4-dihydroxyphenyl)propanoate (f-DA, a fluoro-dopamine)) (Fig. 17)[110]. The energy storage capability of the nanocomposites was greater than that of the neat polymer. At 530 MV m^{-1}, the discharged energy density of the P(VDF-HFP) nanocomposites with 2.5 vol. % of f-PDA-TiO_2 NWs was 11.48 J cm^{-3}, compared to that of the

commercial biaxial oriented polypropylene (3.56 J cm^{-3} at 600 MV m^{-1}).

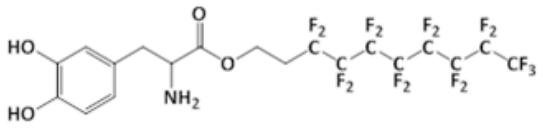

Fig. 17. Structure of the fluoro-dopamine, f-DA

Rosenholm and his team[111] designed a nanocarrier for hydrophilic drugs delivery by combining the adhesive characteristic of polydopamine and the porous structure of mesoporous silica nanoparticles. As known, surface polymerization of dopamine could have occurred through Schiff's base formation and/or by Michael type addition involving quinone groups of the oxidized form of dopamine with the primary amino groups present in the latter dopamine. The average pore size and the diameter of the engendered nanoparticle systems were 4.0 and ~70 nm, respectively. The loading capacities of the as-made nanocarrier for doxorubicin hydrochloride (DOXO) and calcein, the two hydrophilic tested drugs, were 380 and 320 µg mg^{-1}, respectively. Such high loading capacity of the nanocarrier was imputed to the plausible π-π stacking interactions between the aromatic rings of polydopamine and those of drugs.

Silica nanorods (average diameter = 200 nm, average length = 1.5 µm) were employed as templates for devising rod-like nanocapsules from poly(lactide)-b-amidated poly(3,4-dihydroxyphenylalanine) (PLA-b-APDOPA) and polyDOPA (PDOPA) for drug delivery[112]. A self-polymerization of 3,4-dihydroxyphenylalanine in Tris buffer solution in the presence of silica nanorods yielded PDOPA-coated silica, followed by a subsequent coating with (PLA-b-APDOPA). The PLA-b-APDOPA/PDOPA nanocapsules were removed from silica templates using 2 M HF/8 M NH_4F solution at pH 5. PLA-b-APDOPA/PDOPA nanocapsules showed negligible cyctotoxicity to the cells; a concentration of PLA-b-APDOPA/PDOPA nanocapsules of 2 mg mL^{-1} was tested for NIH/3T3 cells, resulting in cell viability of 88%. About 60% of encapsulated ibuprofen, a nonsteroidal anti-inflammatory drug, was released from the PLA-b-APDOPA/PDOPA nanocapsule after 8 h at a pH of 7.4. However, only 10% of ibuprofen was released at a pH of 5.8.

Metal nanoparticles, MNPs

Neoh and his team[113] reported the formation of silver nanoparticles (AgNPs) by reducing silver ions with silicon wafers coated polydopamine or poly(methoxydopamine). The reduced silver ions would bind to catechol units and amine groups of the polydopamine. The methoxyl group on dopamine (DA) was found to accelerate greatly the polymerization of dopamine; a 13 nm thickness of film could be reached within 8 h for 5-methoxydopamine (OMeDA) whereas it took 24 h for unsubstituted dopamine to gain that thickness. The electron-releasing ability of the methoxy group enhanced the oxidation potential of the catechol moiety, therefore accelerating the polymerization. In this work, the one-pot work-up in which the deposition of AgNPs could achieved by incubating Si substrate in a solution containing Ag^+ and the dopamine monomer (DA or OMeDA). The deposited AgNPs proved to be efficient antibacterial systems; indeed, the number of viable S. aureus strains on polydopamine/Si/AgNPs and poly(methoxydopamine)/Si/AgNPs were found to drop by 95 and 100%, respectively, compared to the results with pristine Si wafers.

PDA/Ag nanocomposite particles were accomplished by allowing the aqueous mixture of PDA particles and $[(Ag(NH_3)_2)]^+$ ions to stir for 1 h, a polydopamine-assisted electroless Ag metallization[114]; silver ions were reduced to AgNPs (average diameter = 83 nm) by the catechol units and subsequently bonded to PDA. PDA/Ag nanocomposite and PDA particles exhibited no significant cytotoxicity against the HEK293T human embryonic kidney cells. While PDA particles did not present an anti-bacterial activity *Escherichia coli* and *Staphylococcus aureus*, PDA/Ag nanocomposite particles inhibited their growth. Ou and Li[115] adopted the mussel-inspired strategy to realize silver-based superhydrophobic surfaces (SHS). AgNPs were deposited on PDA-coated SHS (titanium alloy, silicon, polypropylene), by immersion of the coated surface into solution of $[(Ag(NH_3)_2)]^+$ ions and formaldehyde. The surface superhydrophobicity of SHSs was retained upon AgNPs deposition on PDA coatings after exposition to air for 60 days or in contact with water for 70 days; for example, the water contact angle of Si surface decreased slightly, from 171.6° to 166.5°. The PDA-SHS/AgNPs presented excellent anti-bacterial activity against *Escherichia coli* and

Staphylococcus aureus, as a result of the released Ag^+ bactericide and the superhydrophobicity. Xu and his collaborators[116] designed superhydrophobic lotus-leaf-like fabrics (polyethylene terephthalate (PET), PET/cotton, polypropylene (PP), and cotton) by applying a PDA coating, followed by AgNPs deposition and subsequent fluorination with 1H,1H,2H,2H-perfluorodecanethiol. The fluorinated PDA-PET and PDA-PET/AgNPs composite showed water contact angles of 136° and 155°, respectively, and sliding angles lower than 9°, suggesting the superhydrophobic character of the composites and the roles of PDA coating and AgNPs in superhydrophobicity ensuing. The different PDA-Fabric/AgNPs composites were able to separate oil from oil/water mixtures and showed an excellent self-cleaning property.

Poly(dihydroxystyrene-b-styrene) was made by deprotection of the methoxy groups with BBr_3 of poly(dimethoxystyrene-b-styrene) synthesized using RAFT polymerization as illustrated in equation 14[117] The molecular weights M_ns of poly(dimethoxystyrene-b-styrene)s were in the range of (5.10-6.73)×10^4 g mol^{-1} and their polydispersity indexes I_ps fluctuated between 1.19 and 1.25. The poly(dihydroxystyrene-b-styrene) was found to be soluble in DMF and a mixture of chloroform and methanol and insoluble in chloroform, dichloromethane, and THF. AgNPs were fabricated by addition of aqueous $AgNO_3$ solution into a solution of poly(dihydroxystyrene-b-styrene) in a mixture of DMF and chloroform. The strong absorption of the resulting product in the UV-Visible spectrum at 400 nm was assigned to the plasmonic absorption of AgNPs. The average diameter of AgNPs ranged from 6.6 to 10.9 nm and was related to the molecular weight of the copolymer; the higher the molecular weight, the greater the average particle diameter. The same school[118] succeeded in making microphase-separated structures of poly(dihydroxystyrene-b-styrene) films using spin casting; these structures were conceived as templates for the spontaneous creation of silver nanoparticle arrays through the reductive property of catechol units.

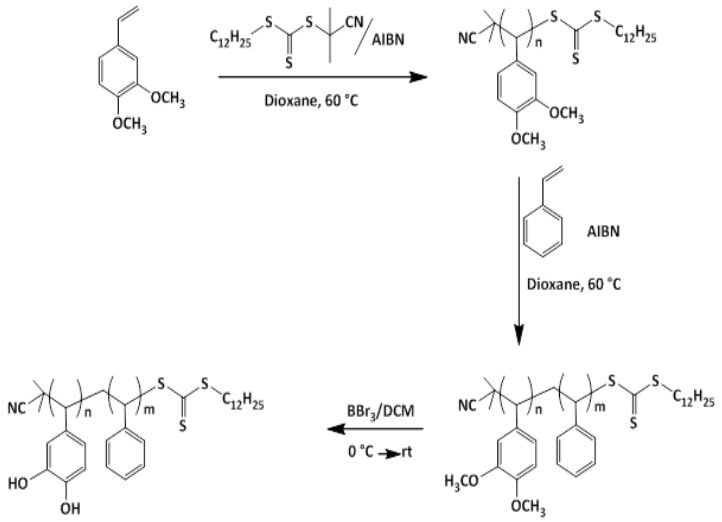

(14)

Tam and his co-workers[119] applied polydopamine coating on cellulose nanocrystals in order to anchor AgNPs on their surfaces. Such a nanosystem served as nanocatalyst for the reduction of nitrophenol into aminophenol using $NaBH_4$ as reducing agent; the catalytic efficiency of this hybrid nanocatalyst was six-fold that of pristine AgNPs. About 4 wt.% of AgNPs (30-90 nm) were deposited on PDA-coated Bombyx mori silk fibroin for antibacterial purposes[120]. In this work, PDA coating was realized at room temperature for 12 h and the AgNPs deposition on the PDA-coated silk was achieved in 8 h at room temperature. The PDA coating did not alter the crystallinity of the silk fibroin. XRD analysis confirmed the uniform distribution of silver nanoparticles. The PDA-coated silk/AgNPs had significant anti-bacterial activity to *E.coli and S. aureus*; whereas the virgin silk fibers and the PDA-coated ones did not.

AgNPs were attached onto electrospun nanofibers from poly(methyl methacrylate-co-dopamine methacrylamide) and the resulting hybrid nanosystem was evaluated for its antibacterial activity, biocompatibility, and wound healing capacity[121]; the size of the attached AgNPs increased with prolonging the incubation time: 18 nm after 6 h, 40 nm after 12 h, and finally 69 nm after 24 h. The same school[122] proved through antibacterial tests that AgNPs were immobilized onto electropolymerized polydopamine in a more efficient manner than those immobilized onto self-polymerized polydopamine (dip-coating); catecholic units of electropolymerized polydopamine were found to be uniformly dispersed on the surface due to the lower surface roughness of the ensued coating.

To enhance the antibacterial activity, the mechanical properties, and the electrical conductivity of cellulose nanofibers, Hwang and his collaborators[123] functionalized carboxylated cellulose nanofibers with dopamine by means of EDC/NHS chemistry, followed by deposition of AgNPs onto their surface by dipping into $AgNO_3$ solution. The anisotropic alignment of the dopamine/AgNP units in the composite, a result of the creation of short-range attractions via hydrogen bonds, hydrophobic interaction, π-π stacking, and quinhydrone charge-transfer complexes, would have induced an enhancement in the sought properties of cellulose nanofibers. UV-Vis spectrum of the nanocomposite showed a surface plasmon resonance absorption peak of AgNPs at 400-440 nm and their size was in the range of 10-90 nm. The mechanical properties of the carboxylated cellulose nanofibers-dopamine conjugate and its composite with AgNPs were greater than those of parent carboxylated cellulose nanofibers. Their stiffness and toughness were 1298 MPa and 2.51 MJ m^{-3}, and 1759 MPa and 3.29 MJ m^{-3}, respectively. The electrical conductivity of the nanocomposite was measured to be ~4 S cm^{-1}, whereas those of carboxylated cellulose nanofibers and carboxylated cellulose nanofibers-dopamine were lower than 10^{-6} S cm^{-1}. The nanocomposite revealed a great antibacterial activity against *E. coli and S. aureus*, whereas no antibacterial activity was noticed for carboxylated cellulose nanofibers.

In the aim at impeding the occurrence of catheter-related bloodstream infections, central venous catheters (CVC) were coated with a polydopamine film which could anchor AgNPs with an average size of 30-50 nm[124]. Polydopamine coating rendered the CVC less hydrophobic and more wettable, as evidenced by the values of its water contact angle θ_w = 80.4°, compared to that of the nascent CVC (θ_w = 113.3°). The AgNPs/polydpamine-coated CVC, formed by dipping polydpamine-coated CVC into 1.0 M solution of $AgNO_3$, was more hydrophilic as suggested by its θ_w = 52.2°. The generated AgNPs/polydopamine-coated CVCs showed high antibacterial activity against *S. aureus* and high cytotoxicity towards the WST-1 cells, and the extents of these properties were found to depend on the AgNPs content.

Hu and his team[125] were able to realize core-shell nanoparticles consisting of Ag ions as core and polyDOPA as shell, by mixing L-DOPA with $AgNO_3$ in alkaline solution; L-DOPA acted as a reducing agent and a stabilizer for silver nanoparticles formation. Such nanosize systems were designed for Hg^{2+} detection (Fig. 18). The Ag/polyDOPA nanoparticles were stable in a pH range of as wide as 3-11 with ionic strength as high as 200 mM NaCl. The catechol entity on the surface ensured the redox property of Ag/polyDOPA nanoparticles which allowed the colorimetric detection of Hg^{2+} via its reduction to Hg^0; a color change from gold yellow of Ag/polyDOPA nanoparticles solution to purple blue one upon addition of Hg^{2+}. With Ag/polyDOPA nanoparticles, the detection of mercury ions was possible even in the presence of other metal ions such as Cr^{3+}, Al^{3+}, Fe^{3+}, Zn^{2+}, Ni^{2+}, and Mn^{2+}. The excellent sensitivity and selectivity of this method were approved by its application in the Hg^{2+} detection in river water and pharmaceuticals and personal care products.

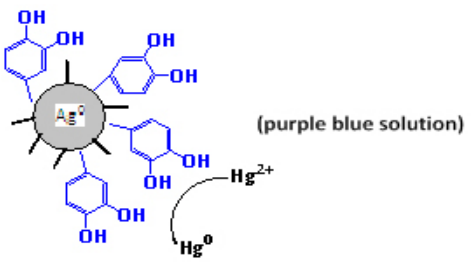

Fig. 18. Detection of mercury ions by reduction with Ag/polyDOPA nanoparticles

A hybrid nanocomposite, involving polydopamine-coated reduced graphene oxide (PDA-rGO) and AgNPs, was conceived as a hydrogen peroxide sensor[126]. PDA-rGO was first made by mixing dopamine and graphene oxide in an aqueous dispersion (Tris-buffer, pH = 8.5); the self-polymerization induced an *in situ* reduction of GO into rGO. The dispersion of PDA-rGO and $AgNO_3$ solutions in the presence of some DA afforded PDA-rGO/AgNPs nanocomposites. The band observed at 430 nm in the UV-Vis spectrum of the nanocomposite was attributed to the surface plasmon resonance absorption of AgNPs. The average particle size of AgNPs was about 100 nm. The cyclovoltametric analysis using a PDA-rGO/AgNP-coated glassy carbon electrode exhibited a linear response in a H_2O_2 concentration range from 5 µM to 8 mM with a detection limit of 2.07 µM.

Gold nanocrystals with branched shapes were demonstrated to grow only in the presence of L-DOPA in alkaline solution and without the aid of nanoseeds[127]; the addition of NaOH is highly critical for the formation of such Au nanoparticles with a mean dimension of 35 nm. L-DOPA reduced the metal ion, resulting in its oxidized forms. The addition of NaOH raised the pH of the medium, promoting a faster reduction rate and the ensued polyDOPA, a product of L-DOPA oxidation, may have coordinated the Au nanoparticle surface, forming a capping layer. The morphology of Au nanocrystals morphology was proven to be L-DOPA concentration-dependent; indeed, star and flower shapes of the Au nanocrystals were detected and the color of the nanoparticles solution shifted from purple to grey on going from 0.03 to 0.27 mM of L-DOPA. Gold nanoparticles (AuNPs)-based catalyst for the reduction of 4-nitrophenol was achieved by mixing an aqueous solution of $HAuCl_4 \bullet 3H_2O$ to an aqueous dispersion of polydopamine-functionalized boron nitride nanosheet[128]; the resulting solution turned pink as a result of reduction of Au^{3+} by the o-benzoquinone units, the oxidized form of the catechol groups of polydopamine. The surface plasmon resonance absorption peak of AuNPs appeared at 540 nm in the UV-Vis spectrum of the nanocomposite and its size was about 8 nm. The catalytic activity of the AuNPs/PDA-functionalized boron nitride nanosheet in the reduction of 4-nitrophenol to aminophenol was greater than those of PDA-functionalized boron nitride nanosheets and PDA-stabilized AuNPs. More than 60% of the catalytic activity of the AuNPs-based nanocomposite could be maintained after five runs.

Messersmith's group[129] designed nanoparticle/metal-organic framework (MOF) core-shell nanohybrids, consisting of polydopamine-coated Au nanoparticle (average diameter = 50 nm) and ZIF-8 (zeolitic imidazole) and UiO-66 crystals as MOFs (= zinc as core, 2-methylimidazole as organic ligand taken as a model for ZIF-8; UiO-66 = zirconium(IV) as core, 1,4-benzenedicarboxylic acid taken as organic ligand) (Fig. 19). AuNPs could be of different morphologies, including nanostar one. The fast nucleation of the crystals, affording well-defined core-shell nanohybrids, was reasoned in terms of the chelating ability of the residual catechol units of PDA and the hydrophobic interaction between its aromatic groups and the organic ligands. The as-made nanohybrids, PDA-AuNPs/ZIF-8 and PDA-AuNPs/UiO-66 were of BET surface areas smaller than of ZIF-8 and UiO-66 crystals, 1082 and 1353 $m^2\ g^{-1}$ against 1541 and 1496 $m^2\ g^{-1}$ (BET = Brunauer-Emmett-Teller). Nanohybrids consisting of polystyrene-trapped magnetic iron oxide nanoparticles (MagNPs), PDA-AuNPs and the above MOFs were prepared and evaluated for their catalytic activity in the reduction of 4-nitrophenol to aminophenol and methylene blue to leuco MB (LMB) by $NaBH_4$. While the MOFs did not shown any catalytic activity in the reduction of 4-nitrophenol, and the nanohybrid MagNPs/PDA-AuNPs without MOF shell led to its rapid conversion, the MagNPs/PDA-AuNPs/ZIF-8 completely inhibited the reaction; the latter inhibition was thought to be due to molecular sieving difference, the size of ZIF-8 (3.4 Å) is smaller than that of the 4-nitrophenol molecule (~4.8 Å). Moreover, the use of UiO-66 as MOF in the nanohybrid, having larger size (6.0 Å), revealed about the same catalytic activity as MagNPs/PDA-AuNPs (~100% after a reaction time of 45 min.), As to the reduction of MB (~7.6 Å), only MagNPs/PDA-AuNPs showed a significant catalytic activity (~100% after a reaction time of 10 minutes).

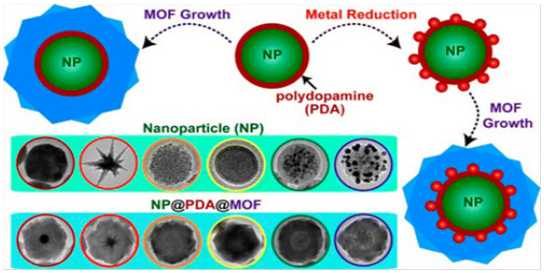

Fig. 19. Nanoparticle/metal-organic framework (MOF) core-shell nanohybrids[129] ("Reprinted (adapted) with permission from (J. Zhou, P. Wang, C. Wang, Y. T. Goh, Z. Fang, P. B. Messersmith, H. Duan, Versatile core-shell nanoparticle@ metal-organic framework nanohybrids: Exploiting mussel-inspired polydopamine for tailored structural integration, ACS Nano 2015, 9(7), 6951-6960.). Copyright (2015) American Chemical Society."

DNA strands were immobilized onto polydopamine-coated AuPNs via Michael addition and/or Schiff base reactions[130]. Dopamine was self-polymerized under alkaline conditions (pH = 8), affording polydopamine that coated 50 nm-AuPNs. The PDA-AuPNs/DNA core-shell nanoparticles were markedly chemically and thermally stable, making them adequate for use in cell imaging. Li and his group[131] developed a nicotine-sensing nanocomposite consisting of PDA-functionalized reduced graphene oxide-gold nanoparticle (PDA-rGO/AuNPs). The surface plasmon resonance absorption of AuNPs in the PDA-rGO/AuNPs nanocomposite appeared at 510 nm in the UV-Vis spectrum, and the average size of gold nanoparticles was 35.7 nm. By means of cyclovoltametry using a PDA-rGO/AuNPs-coated glassy carbon electrode, the low detection of nicotine in tobacco was 0.015 µM and this nicotine sensor showed a linear response range from 0.05 to 500 µM.

Fu and Yu[132] prepared PDA-rGO/PdNPs nanocomposite by mixing PDA-rGO with $PdCl_2$ for 2 h, followed by reaction with $NaBH_4$ for 5 h at room temperature. The nanocomposite was evaluated as an efficient dopamine sensor; indeed, it showed a linear response range from 0.05 to 1 mM and a low detection limit of 6.237 µM. Immersion of polydopamine-functionalized cotton nanofibers in K_2PdCl_4 solution at 0 °C led to deposition of PdNPs layer on their surface[133]. The produced PDA-cotton fibers/PdNPs composite was characterized by scanning electron, microscope Raman spectroscopy, X-ray photoelectron spectroscopy (XPS), microwave plasma-atom emission spectrometer (MP-AES), and energy-dispersive X-ray spectroscopic (EDS). The average size of PdNPs was about 14 nm. The composite was examined for its catalytic activity in a fixed-bed system for the reduction of 4-nitrophenol using $NaBH_4$ as reductant and for Suzuki coupling reaction. In this way, the composite was found to present high activity (turnover frequency, TOF, up to 1.587 min^{-1}), high flow rate (up to 60 mL min^{-1}), and high recyclability (up to 11 cycles) in the reduction reaction of 4-nitrophenol, and high conversion in Suzuki coupling reaction of iodobenzene (up to 96.7%).

Polydopamine-coated cobalt nanoparticles CoNPs (20-38 nm) were embedded in nitrogen-doped reduced graphene oxide (NrGO) matrix in view of enhancing the stability of sulfate radical-based advanced oxidation processes (SR-AOPs), a promising catalyst for degrading water pollutants[134]. The porosity and surface area of as-made PDA-CoNPs/NrGO nanocomposite were measured to be 0.55 $cm^3\ g^{-1}$ and 568.3 $m^2\ g^{-1}$, respectively; those of NrGO were 0.19 $cm^3\ g^{-1}$ and 188.8 $m^2\ g^{-1}$. The higher porosity and surface area would allow a better adsorption and diffusion of the pollutants into the PDA-CoNPs/NrGO matrix. The latter hybrid was demonstrated to be superparamagnetic with a saturation magnetization of 13.51 emu g^{-1}. Besides SEM, HR-TEM, and XPS analyses of the nanohybrid, Raman spectroscopy showed the two characteristic bands of graphene oxide, 1350 cm^{-1} (D band) and 1580 cm^{-1} (G band), with ID/IG of 1.12. PDA-CoNPs/NrGO material was found to efficiently catalyze the oxidative degradation of 4-chlorophenol, a pollutant type, using peroxymonosulfate or oxone ($2KHSO_5 \bullet KHSO_4 \bullet K_2SO_4$); a complete degradation occurred with 120 minutes. The hybrid catalyst retained its catalytic efficiency up to four runs.

Hydroxyapatite nanoparticles, HApNPs

Oil-in-water emulsion (O/W) droplets that were stabilized by phosphorylcholine-poly(cyclooctene) surfactant having pendant catechol units proved to be effective in transporting hydroxyapatite nanoparticles (HApNPs)[135]. The feature of such surfactant was that the NP-droplet interactions and the NPs transport in fluid flow could be induced by the catechol functionality, providing an

adhesive character. The catechol-bearing polymeric surfactant was achieved by copolymerization of pentafluorophenyl ester-containing cyclooctene with phosphorylcholine-substituted cyclooctene via ring-opening metathesis polymerization (ROMP) using a Grubbs catalyst, followed by amidation with dopamine hydrochloride (equation 15). This surfactant (a molecular weight of ~70 kDa) was characterized with an interfacial tension value of ~12.5 mN m^{-1} at the tricholorobenzene/water interface. The designed O/W emulsion stabilized by the surfactant was able to pick up about 99% of HApNPs from the silicon adherend, and 70 to 80 % from polydimethylsiloxane (PDMS) and mica substrates; however, no nanoparticles pick-up was detected for PET (polyethyleneterephthalate) and PEEK (polyether ether ketone) films, suggesting a stronger interaction of the nanoparticles with these substrates.

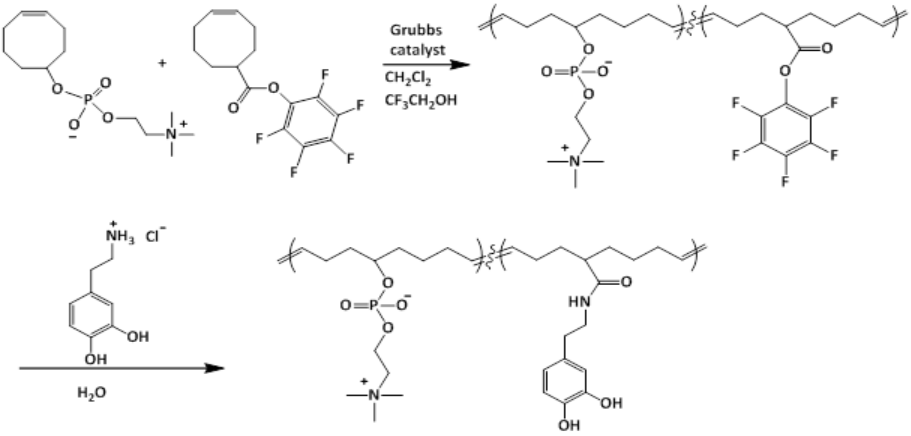

(15)

Cai's research team[136] reported a nanocomposite made of poly(L-lactide) and polydopamine-coated hydroxyapatite nano-rods. The coating of HApNPs with polydopamine proceeded by mixing dopamine hydrochloride with nanoparticles dispersed in Tris solution (pH = 8.5) for 48 h at room temperature. Casting of the mixture solution containing poly(L-lactide) and the PDA-coated HApNPs afforded a nanocomposite film. PDA-coated HApNPs were characterized by X-ray photoelectron spectroscopy (XPS), Fourier transform infrared spectroscopy (FT-IR), Raman spectroscopy, dynamic light scattering (DLS), and scanning electron microscope (SEM). The resulting film presented mechanical properties higher than those of the film from uncoated HApNPs, and a good biocompatibility with bone mesenchymal stem cells, without causing adverse effects on the biological properties. With this polydopamine coating, the interfacial adhesion required for bone engineering was enhanced.

Non-metal nanoparticles (Carbon, sulfur)

Wei's group[137-142] took on the task of functionalizing the carbon allotropes and their derivatives by virtue of the combination of mussel inspired chemistry and radical polymerization. All the below-described functionalized materials were thoroughly characterized by means of FT-IR, XPS, TGA, and TEM. PEGylation of surface of carbon nanotubes (CNTs, 30-50 nm) involved three major steps[137]: 1) PDA coating via self-polymerization of DA in alkaline medium, 2) reaction of PDA-coated CNTs with 2-bromo-2-methylpropionyl bromide, 3) SET-LRP polymerization of poly(ethylene glycol) methyl ether methacrylate (PEGMA) in the presence of CuBr/*tris*[2-(dimethylamino) ethyl] amine (Me_6TREN). The PEGylation degree was given in terms of mass percentage of grafted polymer which was estimated to be about 18%. The PPEGMA-*g*-PDA/CNT showed a better dispersibility in water, DMSO, DMF, and THF for a period of time of 24 hours. The third step was repeated with sodium *p*-styrenesulfonate hydrate (SPSH) and stearyl methacrylate (SMA) to afford hydrophilic PSPSH-*g*-PDA/CNT and hydrophobic PSMA-*g*-PDA/CNT, with the grafting degree of 19.7 and 53.0%, respectively[138]. The dispersibility of CNTs, in water was improved by grafting the hydrophilic PSPSH, as well as in organic

solvents (acetone, DMF and THF) by grafting the hydrophobic PSMA. A thermo-responsive polymer poly(N-isopropylacrylamide) (PNIPAAm) was also tethered on CNTs with about 34% grafting, applying the same protocol[141]. The PNIPAAm-*g*-PDA/CNT showed excellent dispersibility in water for up to 24 h at 25 °C, and in organic solvents (DMF, THF, DMSO). Its thermo-responsiveness was observed as the dispersed system at 25 °C aggregated when heated up to 45 °C and could be redispersed when cooled down to 25 °C. Amine-terminated poly(methacryloxyethyltrimethyl ammonium chloride), NH_2-PDMC, synthesized by chain transfer free radical polymerization using cysteamine hydrochloride as the chain transfer agent, was grafted onto PDA-coated CNTs in Tris buffer solution (pH = 8.5)[139]; the extent of grafting was 22.7 wt.%. The PDMC-*g*-PDA/CNT was dispersible in water for 24 and in organic solvents (THF, DMSO) for 12 h. In the same fashion, aminated-PPEGMA was produced and conjugated to PDA-coated CNTs to an extent of ~15 wt.%[142]. The PPEGMA-PDA/CNT was dispersible in water and acetone for 24 h, and presented good stability in PBS and saline solutions for the same period of time. Its cell viability was found greater than 89% after an incubation time of 24 h, suggesting its compatibility with cells. Another strategy of PEGylation of CNTs adopted by this research group[140] was to anchor the dopamine-modified copolymer of PEGMA and itaconic acid (IA), P(PEGMA-co-IA-DA), onto the surface of CNTs via mussel chemistry, that is at pH = 8.5. An enhanced dispersibility of CNT in water and organic solvents (DMSO and THF) for as long as 12 h was observed upon such PEGylation. A good cytocompatibility of P(PEGMA-co-IA-DA)-modified CNTs was claimed. Wein *et al.,*[143-145] extended their functionalization undertakings of carbon allotropes to graphene oxide but in aqueous solutions. The graphene sheets were exfoliated from graphite by virtue of a modified Hummers' method. Graphene oxide (GO) underwent PEGylation with P(PEGMA-co-IA-DA) under mussel inspired conditions[143]; PEGylation extent was estimated to be 47.46 wt.%. Compared to the nascent GO, the P(PEGMA-co-IA-DA)-GO exhibited a better dispersibility in water and inorganic solvents (DMF, DMSO) for 24 h without deposition. The controlled release of the cis-platinum loaded onto P(PEGMA-co-IA-DA)-GO in the PBS solution was found, after 1 h incubation, ~30 and ~50% at pH of 7.4 and 5.5, respectively. Moreover, the as-devised nanomaterial was not toxic to both HeLa cells and A549 cells; its cell viability exceeded 90%, even at high concentrations. Poly(N-isopropylacrylamide) (PNIPAAm) (M_n = 18954 Da, I_p = 1.12), prepared via RAFT polymerization, was introduced onto PDA-coated GO via Michael addition[144]. The PNIPAAm-PDA/GO exhibited excellent dispersibility in various organic solvents (ethanol, acetone, methanol, DMF and DMSO) and in water, even after 12 hours. As with PNIPAAm-g-PDA/CNT, the PNIPAAm-PDA/GO proved to be thermo-responsive. In another report[145], polyacrylic acid (PAA) (6565 Da), made by RAFT methodology, was attached to PDA/GO via Michael addition reaction. The in-water dispersibility of the PAA-PDA/GO was pH-dependent; at pH of 5, the deposition occurred after only one hour, but the dispersion was maintained for 12 h at pH of 7.

A reduced graphene oxide-based macro ATRP initiator was achieved by self-polymerizing DA-BiBB (BiBB = 2-bromoisobutyryl bromide), an ATRP initiator bearing-dopamine in the presence rGO nanosheets[146]. The macro initiator, rGO/PDA-Br, could promote the SI-ATRP polymerization (surface-initiated atom transfer radical polymerization) of styrene to afford polystyrene-grafted rGO/PDA, rGO/PDA-PS. The Raman analysis provided the ID/IG of the GO, rGO/PDA-Br, and rGO/PDA-PS as 0.87, 0.93, 1.09, respectively, confirming the success of polystyrene grafting. The molecular weight M_n of grafted PS increased with polymerization time: 12 000 g mol^{-1} (12 h), 32 100 g mol^{-1} (24 h), and 62 000 g mol^{-1} (48 h); its I_p was ~1.11. The water contact angle of GO slightly increased from 53° to 57° upon coating with PDA-Br. A further increase in water contact angle to 86° when PS was grafted after 12 h of polymerization. Prolonging the polymerization to 48 h raised the water contact angle to 100°. The rGO/PDA-PS exhibited better dispersibility in organic solvents including DMF, THF, toluene, chloroform, and 1,4-dioxane. The grafted PS resisted to exfoliation because of the strong adhesion of PDA layer to graphene surface.

A nanocomposite-based cancer drug was conceived by functionalizing nanographene oxide with DA and its *in situ* coating with PDA in the presence of an antitumor therapeutic such as cytarabine hydrochloride (Ara) and

hydroxycamptothecin (HCPT); the graphene oxide (GO) underwent a reduction by DA (rGO) and the drug was encapsulated in the PDA-rGO to yield the nanocomposite PDA-rGO/Drug[147]. The optimal loading capacity of Ara and HCPT were 4.5 and 0.38 mg per mg of GO, respectively, and their encapsulation efficiency was 11.3 and 19%, respectively. The extent of Ara release in PBS (pH 6.8) was determined to be 39% within seven days from PDA-rGO/Ara nanocomposite of 4.50 mg mg^{-1} loading capacity of Ara.

A hybrid of PDA-coated rGO and silver nanowires (PDA-GO/AgNW) gave rise to a material for transparent electrodes and optoelectronic devices[148]. The as-fabricated PDA-rGO/AgNW electrodes had a resistance of 63 Ω sq-1 and a transparency of 70.5%. However, those of PDA-rGO film were ~3.46×108 Ω sq^{-1} and 78.2%. The PDA provided an excellent adhesion between the transparent conductive films (TCF) and the substrate, and ensured a long-term stability of PDA-rGO/AgNW TCF.

An enzymatic system-based biosensing electrode was fashioned from 3D-graphene (3DG), CNTs as carrier, and methylene blue as redox mediator, and horseradish peroxidase (HRP)[149]. In this design, HRP was immobilized onto 3DG/MB-CNTs via a self-polymerized PDA linker. The as-made electrode detected H_2O_2 in a wide concentration spectrum (0.2 to 1.1 mM) with a high sensitivity (227.8 mA mM^{-1} cm^{-2}), a low detection limit (58.0 nM), and a fast response. Meng and his co-workers[150] utilized PDA as linker binds Fe_3O_4 nanosheets to the two sides of graphene sheet. To realize the nanoarchitectural system, the PDA-conjugate reduced graphene oxide (PDA-rGO) was prepared and dispersed in ethylene glycol in the presence of $FeCl_3.6H_2O$ and urea. After a work-up, the 3D graphene/carbon/Fe_3O_4 nanosheet arrays were obtained. Such system was featured with outstanding electromagnetic absorption properties; the maximum reflection loss value could have attained -52.8 dB at 9.5 GHz with a sample thickness of 2.7 mm.

The PDA-modified magnetic graphite nanosheets (Fe_3O_4@graphite) were suited for covalent immobilization of *Candida rugosa* lipase[151]. The saturation magnetization values were ~84.57 emu g^{-1} for Fe_3O_4, ~53.09 emu g^{-1} for Fe_3O_4@ graphite nanosheets and ~37.28 emu g^{-1} for Fe_3O_4@ PDA-graphite nanosheets. A rapid response of the Fe_3O_4@PDA-graphite nanosheets to an applied magnetic fields was noticed, implying its facile magnetic separation. The relative activity of the immobilized lipase increased with increasing amount of loaded enzyme and attained about 100% at 350 mg g^{-1} which were obtained for the immobilization time of 5 h and at pH of 7.0.

The nanoparticles of sulfur, a non metal, were made from the HCl treatment of a mixture of aqueous solutions of $Na_2S_2O_3$ and poly(vinylpyrrolidone) as templating agent, and coated with PDA in Tris-HCl buffered aqueous solution[152]. The as-coated sulfur nanoparticles, PDA-SNPs, were evaluated for their electrochemical performance as cathodes. The size of PDA-SNPs was estimated from several to ten hundred nanometers. The PDA-SNPs nanocomposites with 9.5 nm thick PDA film retained a capacity of 385.1 mA h g^{-1}, that is 54% of the initial discharge capacity at 0.5 C (1C = 1670 mA g^{-1}). This electrochemical performance was superior to uncoated SNPs, suggesting the positive effect of PDA coating.

Miscellaneous nanoscaled materials

Cha's school[153] were able to make up mussel-inspired electrospun nanofibers from polycaprolactone (PCL), Fe^{3+}-DOPA complexes, and a recombinant mussel adhesive protein (*rf*p-1); mechanical properties of the nanofibers were expected to be enhanced due to Fe^{3+}-DOPA complexing nature. The recombinant *rf*p-1 (12 decapeptides, molecular mass of 13.6 kDa) was made through *Escherichia coli* bacterium and modified using mushroom tyrosinase as described[9], to afford DOPA-containing mussel adhesive proteins, (m*rf*p-1). The tensile strengths and Young's moduli of the nanofibers (average diameter = 158 nm) from PCL/*rf*p^{-1} (70:30) and PCL/m*rf*p-1 (70:30) were measured to be 7.8 and 10.7 MPa, and 15.3 and 23.4 MPa, respectively. Those of their corresponding Fe(III)-containing nanofibers were greater: 10.7 and 19.4 MPa, and 19.2 and 46.0 MPa. The incorporation of *rf*p-1 into the nanofibers improved cell attachment and proliferation, and the presence of Fe(III)-DOPA complexes did not reveal any detectable cytotoxic and inhibitory effects on

in vitro cell culture. In a continuing work, Cha *et al.,*[154] realized protein nanoparticles from *r*fp-1 and Fe(III)-DOPA complexes to be employed as carrier for drug release system. Fe(III)-DOPA system entailed a pH-responsiveness to the protein nanoparticles. DOPA-modified recombinant fp-1 (m*r*fp-1) proteins and DOXO-loaded ones (80-130 nm) were fabricated by electrospraying technique. About 80-85% of DOXO were released at pH of 6 and after incubation time of 6 h. However, at pH of 8.2, the release extent was lower (30-35%), indicating the pH-responsiveness of the protein nanoparticle. The DOXO-loaded m*r*fp-1 was markedly cytotoxic against the cancer cells; its IC_{50} was found to be 2 μg mL^{-1}, a value twice that of free DOXO.

Spherical-shaped PDA nanoparticles (PDANPs, 86 nm)) were prepared and shielded with photosensitizer-hyaluronic acid conjugate (PS-HA; pheophorbide-A = PS) to provide an anti-cancer therapeutic (PS-HA/PDANPs, 130 nm)[155]. Fe(III) ions were employed as bridge to bind coordinatively to PDA-NPs through hydroxyl and carboxylic groups ones.

PDA nanosheets with thickness of ~10 nm served as framework for self-initiated photografting and photopolymerization (SIPGP) of several vinyl monomers such as styrene (St), 4-vinylpyridine (4VP), *tert*-butyl acrylate (tBuA), methylmethacrylate (MMA), 3-sulfopropyl methacrylate (SPMA), and (N,N-dimethylamino)ethyl methacrylate (DMAEMA), without the use of initiator, to yield polymer brushes and polymer carpets with characteristics shown in Table 1[156]. While the PDA nanosheets promoted biological cell growth and adhesion of fibroblasts, the PDA-based PSPMA carpet showed a cell anti-fouling.

Table 1: Characteristics of PDA-based polymer carpets and Young's moduli E of the corresponding films

Polymer	Thickness (nm)	Θ_w (°)	rms (nm)	E (GPa)
PSt	108	105	3.8	2.5
P4VP	94	54	2.0	-
PtBuA	88	90	4.6	-
PMMA	127	62	2.3	-
PSPMA	83	12	1.5	-
PDMAEMA	80	78	2.5	5.8

A simple method consisting of self-polymerizing DA in the presence of polyethyleneimine PEI (Mn = 600 g mol^{-1}) at ambient temperature and aerobic conditions afforded PDA-PEI fluorescent organic nanoparticles (mean diameter = 100 nm) within 2 h[157]. The driving force for the formation of these nanoparticles was the π-π interaction and the product of the crosslinking of PDA by PEI via Michael addition. These PDA-PEI fluorescent organic nanoparticles were stable in aqueous systems. The hydrodynamic sizes in water and PBS were 159.8 nm with a polydispersity index (PDI) of 0.288, and 213.4 nm with a PDI of 0.252, respectively. The photoluminescence analysis of PDA-PEI nanoparticles in water exhibited an emission peak at 526 nm whose intensity changed with excitation wavelength; an optimal fluorescence was observed with an excitation wavelength of 380 nm and at a pH range of 7-9. The PDA-PEI fluorescent organic nanoparticles were found to be compatible with A549 cells. High cell viability (91-92%) was noted even at their high concentrations and for incubation time up to 72 h. Their IC_{50} values (50% inhibition concentration) were determined to be 802.8 and 1422.9 mg mL^{-1} for 48 and 72 h, respectively. In the same year, Zhao's team[158] reported the realization of PDA-PEI with fluorescence and water-solubility properties. These investigators advanced that Michael addition was the main mechanism by which PDA was coupled with PEI (equation 16). Yellow-green photoluminescence emissions occurred upon irradiation of an aqueous solution of copolymer (λ = 365 nm). A fluorescence quenching of the copolymer was noticed in the presence of transition metals such as Cu^{2+}, Fe^{3+}, and Ni^{2+}, and the quenching was less significant in the presence

of alkali and alkaline earth metals such as K^+, Mg^{2+}, and Ca^{2+}.

Xing and his collaborators[159] fabricated nanosheets from methylacrylated gelatin/ polycaprolactone (MA-G/PCL) and dopamine-N,N'-methylenebisacrylamide conjugate (DA-MBAAm) as crosslinker, for sutureless stomach incision surgery. The MA-G/PCL electrospun nanofibers were grafted and crosslinked with DA-MBAAm in the presence of 2-hydroxy-1-[4-(2-hydroxyethoxy)phenyl]-2-methyl-1-propanone as photoinitiator. The Young's modulus of the thus-grafted and crosslinked nanofibers was greater than that of uncrosslinked MA-G/ PCL, 500 kPa against 420 kPa. The application of the crosslinked nanofibers in healing the stomach incisions was successful.

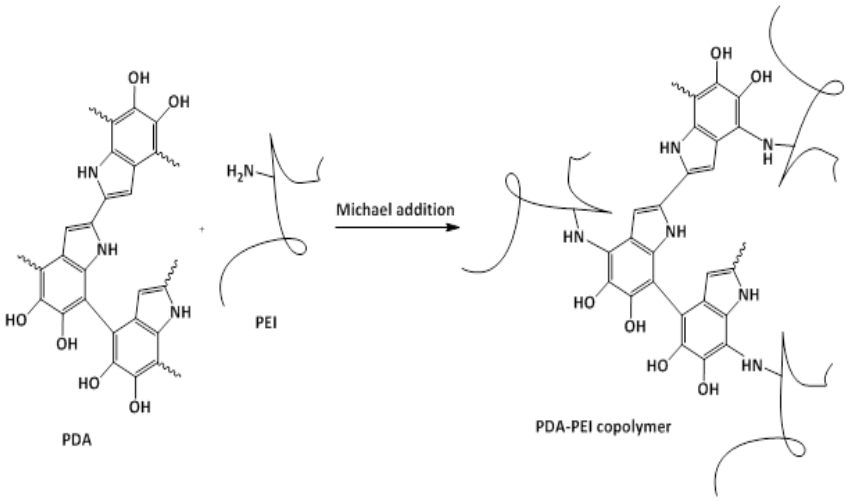

(16)

Kim and his co-workers[160] were able to adhere N-(3,4-dihydroxyphenethyl)-2-mercaptoacetamide molecules on ultraflat gold nanoplates by simple immersion technique. The system consisted of well-ordered self-assembled monolayers of these molecules on the gold nanoplates. The strength of adhesion of the molecules to the gold nanoplates was in the range of 73.78 nN, which was greater than those to annealed Au films (41.55 nN) and evaporated Au film (22.33 nN).

PDA-coated nanosheets, prepared from bulk MoS_2, were functionalized with amino-contained poly(ethylene glycol) methyl ether methacrylate (PEGMEMA) via Michael addition[161]. An extent of about 27% of PEGylation was attained. The PEGMEMA-PDA/MoS_2 nancomposites showed a dispersibility in water far better than MoS_2 in forms of raw material or nanosheets.

Hydrogels with pH-sensitive and magnetic responsive properties were realized by incorporation of iron oxide (Υ-Fe_2O_3) magnetic nanoparticles (MagNPs) into hydrocaffeic acid (HCA)-functionalized chitosan-based gels[162]. At pH 6 and 12, the gelation of HCA-conjugated chitosan (without MagNPs) occurred in the presence of Fe^{3+}, leading to blue-purple and red-colored hydrogels, respectively, with UV-Visible absorbance bands at 550 and 495 nm, indicating the formation of bis- and tris-complexes, respectively. The storage modulus of the gels (without MagNPs) increased from 6 to 20 KPa (at 1 Hz) as the pH of the HCA-chitosan solution was raised from 6 to 12. When the tris-complex hydrogel was treated either with HCl or EDTA, the pH of the gel decreased to 5.5. The storage modulus dropped to ~6.5 and ~3.7 KPa after HCl and EDTA treatments, respectively. Incorporation of Υ-Fe_2O_3 MagNPs (5 wt.%) in the hydrogel led to an increase in the storage modulus to 26 kPa; MagNPs acted merely as fillers and did not react with catechol units. The saturation magnetization of the hydrogel/ MagNPs was measured to be ~0.18 emu g^{-1} against ~0.16 emu g^{-1} for MagNPs.

Jia and Zhu[163] prepared nanocomposite hydrogels (~170 nm) from Laponite and copolymer of N,N'-dimethylacrylamide and comonomers

bearing dopamine (DA) and cholic acid (CA) units (Fig. 20). The latter molecules proved to be indispensable for the formation of hydrogel as no hydrogel could be formed neither with poly(N,N'-dimethylacrylamide) and Laponite only, nor with poly(N,N'-dimethylacrylamide) bearing either dopamine or cholic acid and Laponite; while dopamine secured the adhesion to Laponite, cholic acid moiety helped to self-assemble the system into micelles or aggregates. G' and G" (20 °C) of the nanocomposite hydrogel made of the copolymer (with 2% DA and 2% CA) and Laponite in a mass ratio of 3% were 140 and ~10 Pa, respectively. It was observed that the higher content of DA units may have enhanced the interaction with Laponite, giving rise to a higher stiffness of hydrogels, and that of CA units to a more compact self-assembly; henceforth, the molar fractions of these pendant units would have set the mechanical strength of the resulting hydrogels. The disruption of the as-made hydrogel could be induced by the addition of β-cyclodextrin (β-CD) or Fe^{3+}; the collapse by β-cyclodextrin was the result of the inclusion complexation of the cholic acid units with β-CD, and that by Fe^{3+} was the result of the complexation of catechol with ferric ions (log K_s = 21.63; K_s = complex stability constant).

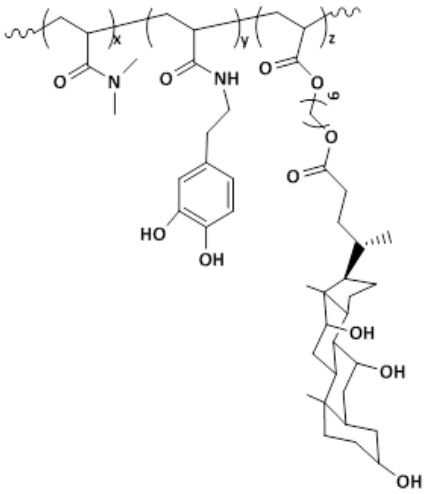

Fig. 20. Copolymer of N,N'-dimethylacrylamide and comonomers bearing dopamine (DA) and cholic acid (CA) units

Lee and his team[164] fabricated nanocomposite hydrogels from dopamine-modified multiarmed PEGs (DA-PEG4, DA-PEG6, and DA-PEG8) (Fig. 21) and Laponite as shape-fitted tissue sealants. While no gel could be formed with DA-PEG4 even after two days and regardless the Laponite concentration, the critical Laponite concentration for the gel formation with DA-PEG6 and DA-PEG8 was 5 wt.%. The rheological parameters G' and G" of the hydrogel from 15 wt.% PEG-D8 and 5 wt.% Laponite, measured at 1 Hz, were found to increase up to ~200 and 50 Pa, respectively, for 20 h of incubation. While the storage modulus G' increased further for 4 days, hinting at an increase in stiffness and cross-linking density, the elastic modulus G" became independent of time, indicating a more elastic behavior of the hydrogel. The hydrogel, incubated for one day, presented a rapid stress relaxation, proving that the strain energy was dissipated via the disassociation of dopamine-Laponite interactions. It was demonstrated that the hydrogel had the ability to be remolded in order to fit the shape of the convex contour of a tissue surface, as a result of formation of intermolecular covalent cross-links.

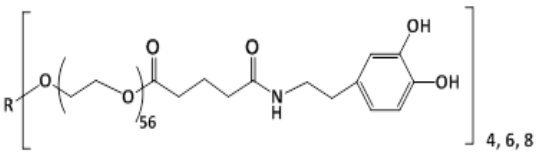

Fig. 21. Dopamine-functionalized multi-armed PEG

Lu and his co-workers[165] constructed an adhesive hydrogel from PDA-intercalated nanoclay and polyacryamide, PDA-Clay/PAAm. The adhesive ability of this hydrogel resided on the amount of free catechol groups of unoxidized DA groups. At 1 Hz, G' of the hydrogel was greater than G", ~150 KPa versus ~40 KPa. This hydrogel was alleged to exhibit excellent adhesion to various surfaces including glass, titanium (Ti), polyethylene (PE), and porcine skin, and to present high extendibility, resilience, and toughness. The remarkable mechanical properties of the hydrogel were imputed to the covalent and noncovalent cross-linking within the nanocomposite. The respective adhesion strengths towards the cited surfaces were 120, 80.8, 80.7, and 28.5 KPa; and such adhesiveness was reproducible and durable even after multiple adhesions or after long-term storage. For example, the adhesion against porcine skin oscillated between 28.5 and ~35 KPa after several adhesion tests. Best of all, the hydrogel could be adhered to human skin and stripped off without causing any irritation or damage. The same investigators[166] developed a conductive, stretchable, self-adhesive, and self-healable hydrogel for cell

bioelectronics. Polymerization of acrylamide (AAm) with ammonium persulfate (APS) in the presence of partially (pGO) or fully reduced (rGO) graphene oxide, prepolymerized DA (PDA), and a crosslinker, afforded the desired hydrogel. Moreover, the integrity of the hydrogel was ensured by the noncovalent interactions taking place between the non-reduced GO and polyacrylamide (PAAm) network via hydrogen bondings and π-π stackings between the catechol groups of PDA and the electrostatic interactions between GO and PAAm. A hydrogel with high performance was obtained with GO/AAm and DA/AAm ratios of 2 and 0.8 wt.%, respectively, and a reaction time of 5 min. between PDA and GO. Under these conditions, the extent of GO reduction was 54%, the conductivity of hydrogel was 0.08 S cm^{-1}, its extension ratio was 35, and its toughness was 4280 J m^{-2}. After a cut, the hydrogel was able to self-heal and to recover a great extent of its mechanical properties (80% of extension ratio, 60% of tensile strength).

Ghavami Nejad and his group[167] reported the realization of nanocomposite hydrogels with an efficient chemo-thermal cancer therapy property via a controlled drug release mechanism. Their strategy was to incorporate a self-polymerized polydopamine nanoparticles (~70 nm) complexed with bortezomib (BTZ) through the boronic acid functionality, into a hydrogel from a copolymer of *N*-isopropylacrylamide (NIPAAm) and acrylamide (AAm). Doxorubicin (DOXO) was also loaded to the PDA-BTZ/poly(NIPAAm-co-AAm) hydrogel by means of an equilibrium partitioning technique. PDA nanoparticles are endowed with photothermal property and cancer drug carrier (BTZ), and BTZ and DOXO are well-known cancer therapeutics; their presence in the nanocomposite hydrogel would engender a synergetic anti-cancer effect. A significant and rapid heating capacity for PDA-BTZ/poly(NIPAAm-co-AAm) hydrogel with higher concentration of PDA was observed upon exposing the sample to an NIR laser (λ = 808 nm). For example, the exposure of the hydrogel containing 400 µg mL^{-1} PDA for 350 s led to a temperature rise to more than 50 °C, a temperature sufficient to kill the cancer cells. This irradiation stimulus provoked a color change, due to the photothermal effect of PDA, indicating that the attained temperature was above the low critical solution transition (LCST) of the hydrogel. Also, the volume and the weight of the hydrogel decreased after laser exposure and could be restored to their original states after laser removal, a good characteristic of drug delivery system. A faster DOXO release from the composite hydrogel took place at pH of 5 and nearly 85% of the drug was delivered to the PBS medium after four cycles of NIR laser exposure (350 s); at pH of 7.4, the DOXO release was about 65%. However, the release BTZ was drastically slower: 68% at pH of 5 and only 20% at pH of 7.4, after 30 h of exposure; at pH 5, a typical acidic cancer environment, there would be decomplexation between BTZ molecules and catechol units of PDA, to liberate more BTZ molecules.

A catalytic degradation of methylene blue was also achieved using gold nanoparticles-deposited polypropylene membrane (AuNP-PP)[168]. The latter composite membrane was realized by reducing chloroauric acid (HAuCl4) with PDA-coated PP membrane. The water permeability of the as-prepared AuNP-PP composite membrane decreased with a polymerization time of dopamine and with increasing dopamine concentration, from 300 L m^{-2} h^{-1} (unmodified PP membrane) to 74 L m^{-2} h^{-1} at a rate of 3.53 L m^{-2} h^{-1} for a reaction time of 24 h and 2.0 mg L^{-1} of dopamine. Up to 85% of methylene blue could be degraded by AuNP-PP membrane.

PDA particles with diameter ranging from 100 to 500 nm, synthesized by self-polymerization of dopamine in alkaline condition (pH = 8.5), were shown to catalyze efficiently the thiol coupling reactions in weakly alkaline, weakly acidic, and neutral aqueous media at room temperature under an aerobic environment[169]. For example, the conversion of the PDA-catalyzed reaction illustrated in equation 17 was 96% at neutral pH and after a reaction time of 24 h, whereas less than 5% conversion was observed in the absence of PDA particles. A biomimetic mechanism was proposed, involving three steps: the first one consisted of the attack of quinone groups of PDA by thiolate anion, giving a thioether adduct; the second step consisted of the attack of this by another thiolate anion, forming a disulfide and a catechol-state dopamine; the third step consisted of oxidization of catechol-state dopamine into o-quinone one by oxygen dissolved in the solution.

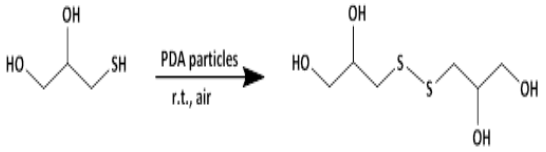

(17)

The mineralization of β-FeOOH nanorods on polydopamine-coated porous fibers, such as polypropylene non-woven (PPNW), polypropylene microfiltration membrane (PPMM), nylon mesh, and polyester cloth, conducted to heterogeneous photo-Fenton catalytic systems that were able to photocatalytically degrade dyes[170]. β-FeOOH nanorods-wrapped PPNW in the presence of H_2O_2 and under visible light degraded methyl blue, methylene blue, rhodamine B, and methyl orange in 40, 55, 65, and 70 min., respectively. All the remaining β-FeOOH nanorods-wrapped substrates exhibited similar catalytic activity towards all dyes. PDA scavenged electrons and reduced the photogenerated electron-hole recombination rate upon reaction of β-FeOOH nanorods with H_2O_2, producing hydroxyl radicals. The efficiency of the β-FeOOH nanorods-wrapped substrates in the decomposition of dyes was higher than 90% after five runs.

Dai and his group[171] modified poly(N-(4-aminophenyl) methacrylamide-co-polyethylene glycol monomethyl ether methacrylate) (P(APMAAm-co-MAPEG)) through Schiff base reaction with 3,4-dihydroxybenzaldehyde as depicted in equation 18. Different nanoassemblies in form of either solid particles, homogeneous vesicles, and Janus vesicles, could have resulted from catechol-metal ion supramolecular coordination involving the thus-functionalized catechol/P(APMAAm-co-MAPEG) and metal ion such as Fe^{3+} and Cu^{2+}. Such nanoassemblies were prone to disassembling in the presence of protein such as BSA and trypsin as evidenced by UV-visible analysis. For example, the bands of catechol/P(APMAAm-co-MAPEG)-Fe^{3+} disappeared upon addition of BSA and two new bands at 275 and 366 nm appeared, assigned to BSA-Fe^{3+} complex; the intensities of these bands increased by increasing BSA concentration.

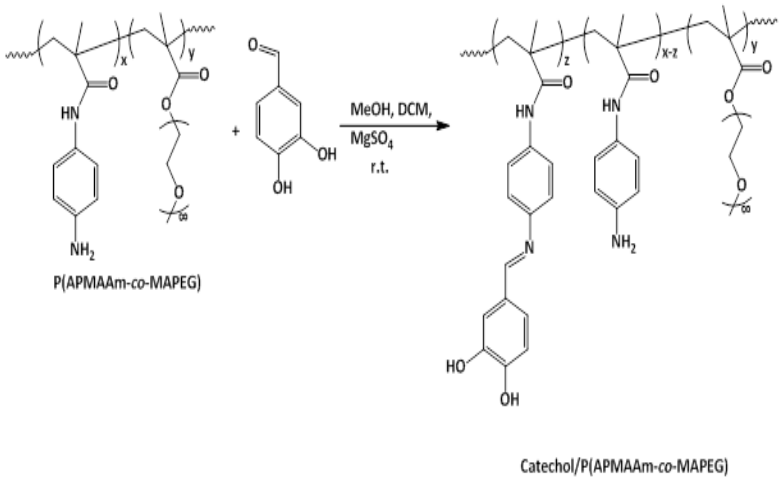

(8)

CONCLUSION

Unveiling of the unique bioadhesiveness of the mussel foot proteins in wet environment has indeed opened a boundless avenue in research. The benefits in understanding the antifouling phenomenon and making nanocomposites in a robust and easy way have indubitably been concretized. Self-polymerization of dopamine and its analogues in alkaline conditions was of a great aid in achieving the mussel-inspired applications and undertakings. The adhesion strength of the newly-made mussel-inspired polymeric materials to some substrates outweighed the commonly used glues: Krazy (super glue or cyanoacrylate), epoxy resin glue, and Elmer's glue. Treatment of a variety of nanoparticles with catechol-containing polymers has served to facilitate the design of items in tune with the desired applications, namely medical ones.

REFERENCES

1. Waite, J. H., Tanzer, M. L., Polyphenolic substance of Mytilus edulis: Novel adhesive containing L-dopa and hydroxyproline, *Science.,* **1981**, *212*, 1038-1040.
2. Waite, J. H., Reverse engineering of bioadhesion in marine mussels, Ann. N. Y. *Acad. Sci.*, **1999**, *875*, 301-309.
3. Yu. M , Hwang J., Deming T. J., Role of L-3,4-dihydroxyphenylalanine in mussel adhesive proteins, *J. Am. Chem. Soc.*, **1999**, *121*(24), 5825-5826.
4. Waite J. H., Adhesion a la moule, Integr. *Comp. Biol.*, **2002**, *42*,1172-1180.
5. Meng H., Liu Y., Cencer M., Lee B. P., Adhesives and coatings inspired by mussel adhesive proteins, in: Bioadhesion and Biomimetics From Nature to Applications, Bianco-Peled H. and Davidovich-Pinhas M. (Editors), *Stanford Pan.*, **2015**, *6*, 131-166.
6. Krogsgaard M., Nue V., Birkedal H., Mussel-inspired materials: Self-healing through coordination chemistry, *Chem. Eur. J.*, **2016**, *22*(3), 844-857.
7. Mian S. A., Khan Y., The adhesion mechanism of marine mussel foot protein: Adsorption of L-Dopa on α- and β-cristobalite silica using density functional theory, *J. Chem.*, **2017**, *6* Article ID 8756519.
8. Nicklisch S. C. T., Waite J. H., Mini-review: The role of redox in dopa-mediated marine adhesion, *Biofouling.,* **2012**, *28*, 865-877.
9. Moulay S., Dopa/catechol-tethered polymers: Bioadhesives and biomimetic adhesive materials, *Polym. Rev.*, **2014**, *54*(3), 436-513.
10. Maier G. P, Rapp M. V., Waite J. H., Israelachvili J. N., Butler A., Adaptive synergy between catechol and lysine promotes wet adhesion by surface salt displacement, *Science.,* **2015**, *349*, 628-632.
11. Forooshani P. K., Lee B. P., Recent approaches in designing bioadhesive materials inspired by mussel adhesive protein, *J. Polym. Sci.*, *Part A: Polym. Chem.*, **2017**, *55*(1), 9-33.
12. Li Y., Liao M., Zhou J., Catechol-cation adhesion on silica surfaces: molecular dynamics simulations, *Phys. Chem. Chem. Phys.,* **2017**, *19*(43), 29222-29231.
13. Mirshafian R., Wei W., Israelachvili J. N., Waite J. H., α,β-Dehydro-Dopa: A hidden participant in mussel adhesion, *Biochemistry.,* **2016**, *55*(5), 743-750.
14. Zhang W., Yang H., Liu F., Chen T., Hu G., Guo D., Hou Q., Wu X., Su Y., Wang J., Molecular interactions between DOPA and surfaces with different functional groups: A chemical force microscopy study, *RSC Adv.*, **2017**, *7*, 32518-32527.
15. Waite J. H., Mussel adhesion-essential footwork, *J. Exp. Biol.*, **2017**, *220*(4), 517-530.
16. Kaushik N. K., Kaushik N., Pardeshi S., Sharma J. G., Lee S. H., Choi E. H., Biomedical and clinical importance of mussel-inspired polymers and materials, Mar. *Drugs.,* **2015**, *13*(11), 6792-6817.
17. Wei Q., Haag R., Universal polymer coatings and their representative biomedical applications, Mater. *Horiz.*, **2015**, *2*, 567-577.
18. Perikamana S. K. M., Lee. J., Lee Y. B., Shin Y. M., Lee E. J., Mikos A. G., Shin H., Materials from mussel-inspired chemistry for cell and tissue engineering applications, *Biomacromolecules.,* **2015**, *16*(9), 2541-2555.
19. Choi B. H., Kim B. J. , Kim C. S., Lim S., Yang.B., Seo J. H. , Cheong H., Cha.H. J. , Mussel-derived bioadhesives. In: Kim SK. (eds), Handbook of Marine Biotechnology. Springer, Berlin, Heidelberg., **2015.**
20. Park K. H., Seong K.-Y., Yang S. Y., Seo S., Advances in medical adhesives inspired by aquatic organisms' adhesion, *Biomater. Res.***2017**, *21*, 16, pp9. DOI 10.1186/s40824-017-0101-y.
21. Cheah Y. S., Santhanakrishnan.S., Sullivan M. B., Neoh K. G., Chai C. L. L., The chemical reactivities of DOPA and dopamine derivatives and their regioselectivities upon oxidative nucleophilic trapping, *Tetrahedron* **2016**, *72*(41), 6543-6550.
22. Hamada V. A., Roman V. A., Howell S. M., Wilker J. J., Examining potential active tempering of adhesive curing by marine mussels, *Biomimetics.,* **2017**, *2*(16), 11 doi:10.3390/biomimetics2030016.
23. Desmond K. W., Zacchia N. A., Waite J. H., Valentine M. T., Dynamics of mussel plaque detachment. *Soft Matter.,* **2015**, *11*, 6832-6839.
24. Filippidi E., DeMartini D. G., de Molina P. M., Danner E. W., Kim , Helgeson M. E., Waite J. H., J. H. Valentine J. H., The microscopic

network structure of mussel (Mytilus) adhesive plaques. *J. R. Soc. Interface.,* **2015**, 12, 20150827.

25. Priemel T., Degtyar E., Dean M. N., Harrington M. J., Rapid self-assembly of complex biomolecular architectures during mussel byssus biofabrication. *Nat. Commun.*, **2017**, *8*, 14539.
26. Daly W. H., Moulay S., Synthesis of polyvinylcatechols, *J. Polym. Sci. Polym. Symp.*, **1986**, *74*, 227-242.
27. Moulay S., Dihydroxybenzene/benzoquinone-containing polymers: Organic redox polymers, L'Actualité Chimique, 12-27, Juillet-Août **2000**.
28. Moulay S., Polymers with dihydroxy/dialkoxybenzene moieties, *C. R. Chim.*, **2009**, *12*(5), 577-601.
29. Takeshima H., Satoh K., Kamigaito M., Bio-based functional styrene monomers derived from naturally occurring ferulic acid for poly(vinylcatechol) and poly(vinylguaiacol) via controlled radical polymerization, *Macromolecules.,* **2017**, *50*(11), 4206-4216.
30. Zhan K., Ejima H., Yoshie N., Antioxidant and adsorption properties of bioinspired phenolic polymers: A comparative study of catechol and gallol, *ACS Sustainable Chem. Eng.*, **2016**, *4*(7), 3857-3863.
31. Oh D. X., Kim S., Hwang D. S., Tunicate-mimetic nanofibrous hydrogel adhesive with improved wet adhesion, *Acta Biomater.*, **2015**, *20*, 104-112.
32. Lee F., Chung J. E., Xu K., Kurisawa M., Injectable degradation resistant hyaluronic acid hydrogels crosslinked via the oxidative coupling of green tea catechin, *ACS Macro Lett.*, **2015**, *4*(9), 957-960.
33. Sedó v, Saiz-Poseu J., Busqué F., Ruiz-Molina D., Catechol-based biomimetic functional materials, *Adv. Mater.*, **2013**, *25*(5), 653-701.
34. Zamiraei Z., Nabid M. R., HRP-catalyzed synthesis of water-soluble and redox poly(catechol) at room temperature, *Chem. Biol. Interface.,* **2015**, *5*(2), 151-156.
35. Mejia-Caballero A., de Anda R., Hernandez-Chavez G., Rogg S., Martinez A., Bolívar F., Castaño V. M., Gosset G., Biosynthesis of catechol melanin from glycerol employing metabolically engineered *Escherichia coli*, *Microb. Cell. Fact.*, **2016**, *15*, 161, 8 p. DOI 10.1186/s12934-016-0561-0.
36. Jenkins C. L., Meredith H. J., Wilker J. J., Adhesives inspired by marine mussels, in Biomaterials from Nature for Advanced Devices and Therapies, Editors: Nuno M. Neves, Rui L. Reis; Hoboken, New Jersey : John Wiley & Sons, *Inc.*, **2016**, 629-650.
37. Li L., Zeng H., Marine mussel adhesion and bio-inspired wet adhesives, *Biotribology .,* **2016**, *5*, 44-51.
38. Hu H., Dyke J. C., Bowman B. A., Ko C.-C., You W., Investigation of dopamine analogues: Synthesis, mechanistic understanding, and structure-property relationship, *Langmuir.,* **2016**, *32*, 9873-9882.
39. Lim C., Huang J., Kim S., Lee S., Zeng H., Hwang D. S., Nanomechanics of poly(catecholamine) coatings in aqueous solutions, *Angew Chem. Int. Ed. Engl.*, **2016**, *55*(10), 3342-3346.
40. Zhang W., Pan Z., Yang F. K., Zhao B., A facile in situ approach to polypyrrole functionalization through bioinspired catechols, *Adv. Funct. Mater.*, **2015**, 10 DOI: 10.1002/adfm.201403115.
41. North M. A., Del Grosso C. A., Wilker J. J., High strength underwater bonding with polymer mimics of mussel adhesive proteins, *ACS Appl. Mater. Interfaces.,* **2017**, *9*(8), 7866-7872.
42. Krysiak S., Wei Q., Rischka K., Hartwig A., Haag R., Hugel Th., Adsorption mechanism and valency of catechol-functionalized hyperbranched polyglycerols, *Beilstein J. Org. Chem.*, **2015**, *11*, 828-836.
43. Rodriguez N. R. M., Das S., Kaufman Y., Israelachvili J. N., Waite J. H., Interfacial pH during mussel adhesive plaque formation, *Biofouling.,* **2015**, *31*(2), 221-227.
44. Wang Y.-Z., F.-S, L. Li. , Du, Li Z.-C., A facile approach to catechol containing UV dismantlable adhesives, *Polymer.,* **2015**, *68*, 270-278.
45. Hiraishi N., Kaneko D., Taira S., Wang S., Otsuki M., Tagami J., Mussel mimetic, bioadhesive polymers from plant derived materials, *J. Investig. Clin. Dent.*, **2015**, *6*(1), 59-62.
46. Wilker J. J., Positive charges and underwater adhesion, *Science.,* **2015**, *349*(6248), 582-583.

47. Brennan M. J., Meredith H. J., Jenkins C. L., Wilker J. J., Liu J. C., Cytocompatibility studies of a biomimetic copolymer with simplified structure and high-strength adhesion, *J. Biomed. Mater. Res.*, A. **2016**, *104*(4), 983-990.
48. Jenkins C. L., Siebert H. M., Wilker J. J., Integrating mussel chemistry into a bio-based polymer to create degradable adhesives, *Macromolecules.,* **2017**, *50*(2), 561-568.
49. Meredith J. J., Wilker J., The interplay of modulus, strength and ductility in adhesive design using biomimetic polymer chemistry, *Adv. Funct. Mater.*, **2015**, *25*(31), 5057-5065.
50. Mu Y., Wan X., Simple but strong: A mussel-inspired hot curing adhesive based on polyvinyl alcohol backbone, Macromol. *Rapid Commun.*, **2016**, *37*(6), 545-50.
51. Brennan J., Kilbride B., Wilker J., Liu J., A bioinspired elastin-based protein for a cytocompatible underwater adhesive, *Biomaterials.*, **2017**, *124*, 116-125. Catechol 35 2017.
52. Yang J., Keijsers J., van Heek M., Stuiver A., Stuart M. A. C., Kamperman M., The effect of molecular composition and crosslinking on adhesion of a bio-inspired adhesive, *Polym. Chem.*, **2015**, *6*(16), 3121-3130.
53. Lee S. B., González-Cabezas C., Kim K. M., Kim K. N., Kuroda K., Catechol-functionalized synthetic polymer as a dental adhesive to contaminated dentin surface for a composite restoration, *Biomacromolecules.,* **2015**, *16*, 2265-2275.
54. Seo S., Das S., Zalicki P. J., Mirshafian R., Eisenbach C. D., Israelachvili J. N., Waite J. H., Ahn B. K., Microphase behavior and enhanced wet-cohesion of synthetic copolyampholytes inspired by a mussel foot protein, *J. Am. Chem. Soc.*, **2015**, *137*(29), 9214-9217.
55. Ahn B. K., Das S., Linstadt R., Kaufman Y., Martinez-Rodriguez N. R., Mirshafian R., Kesselman E., Talmon Y., Lipshutz B. H., Israelachvili J. N., Waite J. H., High-performance mussel-inspired adhesives of reduced complexity, *Nat. Commun.*, **2015**, *6*, 8663. DOI: 10.1038/ncomms9663.
56. Zhao Q., Lee D. W., Ahn B. K., Seo S., Kaufman Y., Israelachvili J. N., Waite J. H., Underwater contact adhesion and microarchitecture in polyelectrolyte complexes actuated by solvent exchange, *Nature Materials.,* **2016**, *15*, 407-412.
57. Wei W., Yu J., Gebbie M. A., Tan Y., Rodriguez N. R. M., Israelachvili J. N., Waite J. H., Bridging adhesion of mussel-inspired peptides: role of charge, chain length, and surface type, *Langmuir.,* **2015**, *31*(3), 1105-1112.
58. Ji Y., Ji T., Liang K., Zhu L., Mussel-inspired soft-tissue adhesive based on poly(diol citrate) with catechol functionality, *J. Mater. Sci. Mater. Med.*, **2016**, (*27*)30, 9.
59. Yi M., Sun H., Zhang H., Deng X., Cai Q., Yang X., Flexible fiber-reinforced composites with improved interfacial adhesion by mussel-inspired polydopamine and poly(methyl methacrylate) coating, *Mater. Sci. Eng. C Mater. Biol. Appl.,* **2016**, *58*, 742-749.
60. Lee W., Lee J. U., Byun J. H., Catecholamine polymers as surface modifiers for enhancing interfacial strength of fiber-reinforced composites, *Compos. Sci. Technol.*, **2015**, *110*, 53-61.
61. Damodaran V. B., Murthy N. S., Bio-inspired strategies for designing antifouling biomaterials, Biomater. Res. 2016, 20, 18, pp11. DOI 10.1186/s40824-016-0064-4.
62. Xu L. Q., Pranantyo D., Ng Y. X., Teo S. L.-M., Neoh K.-G., Kang E.-T., Fu G. D., Antifouling coatings of catecholamine copolymers on stainless steel, *Ind. Eng. Chem. Res.*, **2015**, *54*(22), 5959-5967.
63. Patil N., Falentin-Daudré C., Jérôme C., Detrembleur C., Mussel-inspired protein-repelling ambivalent block copolymers: controlled synthesis and characterization, *Polym. Chem.*, **2015**, *6*(15), 2919-2933.
64. Xu L. Q., Pranantyo D., Neoh K.-G., Kang E.-T., Teo .S. L.-M., Fu G. D., Synthesis of catechol and zwitterion-bifunctionalized poly(ethylene glycol) for the construction of antifouling surfaces, *Polym. Chem.*, **2016**, *7*(2), 493-501.
65. Xu L., Pranantyo D., Neoh K.-G., Kang E.-T., Tea stains-inspired antifouling coatings based on tannic acid-functionalized agarose, *ACS Sustainable Chem. Eng.*, **2017**, *5*(4), 3055-3062.

66. Ding X., Hedrick J. L., Yang C., Yang Y., Antimicrobial and antifouling catechol-containing polycarbonates for medical applications, US Patent., **2015**/0098976 A1.
67. Louzao I., Sui C., Winzer K., Fernandez-Trillo F., Alexander v, Cationic polymer mediated bacterial clustering: Cell-adhesive properties of homo- and copolymers, *Eur. J. Pharm. Biopharm.*, **2015**, *95*(A), 47-62.
68. Yang W., Sundaram H. S., Ella J.-R., He N., Jiang S., Low-fouling electrospun PLLA films modified with zwitterionic poly(sulfobetaine methacrylate)-catechol conjugates, *Acta Biomaterialia.,* **2016**, *40*, 92-99.
69. Liu C.-Y., Huang C.-J., Functionalization of polydopamine via the aza-Michael reaction for antimicrobial interfaces, *Langmuir.,* **2016**, *32*(19), 5019-5028.
70. Dang Y., Quan M., Xing C.-M., Wang Y.-B., Gong Y.-K., Biocompatible and antifouling coating of cell membrane phosphorylcholine and mussel catechol modified multi-arm PEGs, *J. Mater. Chem.*, B **2015**, *3*(11), 2350-2361.
71. Dang Y., Xing C.-M., Quan M., Wang Y.-B., Zhang S.-P., Shi S.-Q., Gong Y.-K., Substrate independent coating formation and anti-biofouling performance improvement of mussel inspired polydopamine, *J. Mater. Chem.*, B **2015**, *3*(20), 4181-4190.
72. Xue v, Cao H., Meng F., Quan M., Gong Y.-K., Cell membrane mimetic coating immobilized by mussel-inspired adhesion on commercial ultrafiltration membrane to enhance antifouling performance, *J. Membr. Sci.*, **2017**, *528*, 1-11.
73. Wang R., Song X., Xiang T., Liu Q., Su B., Zhao W., Zhao C., Mussel-inspired chitosan-polyurethane coatings for improving the antifouling and antibacterial properties of polyethersulfone membranes, Carbohydr. *Polym.*, **2017**, *168*, 310-319.
74. Kang T., Banquy X., Heo J., Lim C., Lynd N. A., Lundberg P., Oh D. X., Lee H.-K., Hong Y.-K., Hwang D. S., Waite J. H., Israelachvili J. N., Hawker C. J., Mussel-inspired anchoring of polymer loops that provide superior surface lubrication and antifouling properties, *ACS Nano.*, **2016**, *10*(1), 930-937.
75. Li L., Yan B., Zhang L., Tian Y., Zeng H., Mussel-inspired antifouling coatings bearing polymer loops, *Chem. Commun*. **2015**, DOI: 10.1039/c5cc06852e
76. Ju Y., Cui J., Muellner M., Suma T., Hu M., Caruso F., Engineering low-fouling and pH degradable capsules through the assembly of metal-phenolic networks, *Biomacromolecules* **2015**, *16*(3), 807-814.
77. Cho Y., Seo S.Y., Park B. J., Joung Y. K., Han D. K., Silicone rubber with mussel-inspired adhesive coatings for enhancing antifouling property and blood compatibility, *Macromol. Res.*, **2017**, *25*(8), 841-848.
78. Pi J.-K., Yang H.-C., Wan L.-S., Wu J., Xu Z.-K., Polypropylene microfiltration membranes modified with TiO_2 nanoparticles for surface wettability and antifouling property, *J. Membr. Sci.*, **2016**, *500*, 8-15.
79. Zhang C., Li H.-N., Du Y., Ma M.-Q., Xu Z.-K., $CuSO_4/H_2O^{2-}$Triggered polydopamine/poly(sulfobetaine methacrylate) coatings for antifouling membrane surfaces, *Langmuir.,* **2017**, *33*(5), 1210-1216.
80. Xiang Y., Liu F., Xue L., Under seawater superoleophobic PVDF membrane inspired by polydopamine for efficient oil/sea water separation, *J. Membr. Sci.*, **2015**, *476*, 321-329.
81. Ling D., Lee N., Hyeon T., Chemical synthesis and assembly of uniformly sized iron oxide nanoparticles for medical applications, *Acc. Chem. Res.*, **2015**, *48*(5), 1276-1285.
82. Gu X., Zhang Y., Sun H., Song X., Fu C., Dong P., Mussel-inspired polydopamine coated iron oxide nanoparticles for biomedical application, *J. Nanomater.*, **2015**, *2015*, Article ID 154592, 12.
83. Burnand D., Monnier C. A., Redjem A., Schaefer M., Rothen-Rutishauser B., Kilbinger A., Petri-Fink A., Catechol-derivatized poly(vinyl alcohol) as a coating molecule for magnetic nanoclusters, *J. Magn. Magn. Mater.*, **2015**, *380*, 157-162.
84. GhavamiNejad A., Sasikala A. R. K., Unnithan A. R., Thomas R. G., Jeong Y. Y., Vatankhah-Varnoosfaderani M., Stadler F. J., Park C. H., Kim C. S., Mussel-inspired electrospun smart magnetic nanofibers for hyperthermic chemotherapy, *Adv. Funct. Mater.*, **2015**, 9, DOI: 10.1002/adfm.201500389.

85. Sasikala A. R. K., GhavamiNejad A., Rajan Unnithan A. R., Thomas R. G., Moon M., Jeong Y. Y., Park C. H., Kim C. S., Smart magnetic nanoplatform for synergistic anticancer therapy by maneuvering the mussel-inspired functional magnetic nanoparticles for pH responsive anticancer drug delivery and hyperthermia, Nanoscale **2015**, DOI: 10.1039/C5NR05844A.
86. Zhou J., Wang C., Wang P., Messersmith P. B., Duan H., Multifunctional magnetic nanochains: Exploiting self-polymerization and versatile reactivity of mussel-inspired polydopamine, *Chem. Mater.*, **2015**, *27*, 3071-3076.
87. Deng X., Cao S., Li N., Wu H., Smith. Th. J., Zong M., Lou W., A magnetic biocatalyst based on mussel-inspired polydopamine and its acylation of dihydromyricetin, *Chinese J. Catal.*, **2016**, *37*, 584-595.
88. Stephen Z. R., Dayringer C. J., Lim v, Revia R. A., Halbert M. V., Jeon M., Bakthavatsalam A., Ellenbogen R. G., Zhang M., Approach to rapid synthesis and functionalization of iron oxide nanoparticles for high Gene transfection, *ACS Appl. Mater. Interfaces.,* **2016**, *8*(10), 6320-6328.
89. Li Q., Barrett D. G., Messersmith P. B., Holten-Andersen N., Controlling hydrogel mechanics via bio-Inspired polymer-nanoparticle bond dynamics, *ACS Nano.*, **2016**, *10*(1), 1317-1324.
90. Li P., Chevallier P., Ramrup P., Biswas D., Vuckovich D., Fortin M.-A., Oh J. K., Mussel-inspired multidentate block copolymer to stabilize ultrasmall superparamagnetic Fe3O4 for magnetic resonance imaging contrast enhancement and excellent colloidal stability, *Chem. Mater.*, **2015**, *27*(20), 7100-7109.
91. Lu C., Park M. K., Lu C., Lee Y. H., Chai K. Y., A mussel-inspired chitooligosaccharide based multidentate ligand for highly stabilized nanoparticles, *J. Mater. Chem.,* B **2015**, *3*(18), 3730-3737.
92. Zhang Q., Nurumbetov G., Simula A., Zhu C., Li M., Wilson P., Kempe K., Yang B., Tao L., Haddleton D. M., Synthesis of well-defined catechol polymers for surface functionalization of magnetic nanoparticles, *Polym. Chem.*, **2016**, *7*, 7002-7010.
93. Yang Y., Wang J., Wu F., Ye G., Yi R., Lu Y., Chen Jing, Surface-initiated SET-LRP mediated by mussel-inspired polydopamine chemistry for controlled building of novel core-shell magnetic nanoparticles for highly-efficient uranium enrichment, *Polym. Chem.*, **2016**, *7*(13), 2427-2435.
94. Zhang L., Li L., Dang Z. M., Bio-inspired durable, superhydrophobic magnetic particles for oil/water separation, *J. Colloid Interface Sci.*, **2016**, *463*, 266-271.
95. Becker G., Ackermann L.-M., Schechtel E., Klapper M., Tremel W., Wurm F. R., Joining two natural motifs: Catechol-containing poly(phosphoester)s, *Biomacromolecules.,* **2017**, *18*(3), 767-777.
96. Lee Y.-K., Lee S.-Y., Mussel-inspired bolaamphiphile sticky self-assemblies for the preparation of magnetic nanoparticles, Colloids and Surfaces B: *Biointerfaces.,* **2015**, *127*, 89-95.
97. Li F., Du M., Zheng Q., Dopamine/silica nanoparticle assembled, microscale porous structure for versatile superamphiphobic coating, *ACS Nano.,* **2016**, *10*(2), 2910-2921.
98. Heng C., Liu M., Wang K., Zheng X., Huang H., Deng F., Hui J., Zhang X., Wei Y., Fabrication of silica nanoparticle based polymer nanocomposites via a combination of mussel inspired chemistry and SET-LRP, *RSC Adv.*, **2015**, *5*(111), 91308-91314.
99. Heng C., Liu M., Wang K., Deng F., Huang H., Wan Q., Hui J., Zhang X., Wei Y., Biomimic preparation of highly dispersible silica nanoparticles based polymer nanocomposites, *Ceram. Int.*, **2015**, *41*, 15075-15082.
100. Tian J. W., Zhang H. X., Liu M. Y., Deng F. J., Huang H. Y., Wan Q., Li Z., Wang K., He X. H., Zhang X. Y., Wei Y., A bioinspired strategy for surface modification of silica nanoparticles, *Appl. Surf. Sci.*, **2015**, *357*, 1996-2003.
101. Huang Q., Liu L., Zeng G., Liu M., Mao L., Huang H., Deng F., Zhang X., Wei Y., Preparation of silica nanoparticle based polymer composites via mussel inspired chemistry and their enhanced adsorption capability towards methylene blue, *RSC Adv.*, **2016**, *6*, 85213-85221.
102. Heng C., Liu M., Wang P., Wang K., Zheng X., Fan D., Hui J., Zhang X., Wei Y., Preparation of silica nanoparticles based multifunctional therapeutic systems via one-step mussel inspired modification, *Chem. Eng. J.* **2016**, 296, 268-276.

103. Huang Q., Liu M., Chen J., Wang K., Xu D., Deng F., Huang H., Zhang X., Wei Y., Mussel inspired preparation of functional silica nanocomposites for environmental adsorption applications, *Appl. Surf. Sci.,* **2016**, *387*, 285-293.
104. Huang Q., Liu M., Guo R. Mao, L., Wan Q., Zeng G., Huang H., Deng F., Zhang X., Wei Y., Facile synthesis and characterization of poly(levodopa)-modified silica nanocomposites via self-polymerization of levodopa and their adsorption behavior toward Cu^{2+}, *J. Mater. Sci.*, **2016**, *51*(21), 9625-9637.
105. Wang C. X., Braendle A., Menyo M. S., Pester C. W., Perl E. E., Arias I., Hawker C. J., Klinger D., Catechol-based layer-by-layer assembly of composite coatings: a versatile platform to hierarchical nano-materials, *Soft Matter.,* **2015**, *11*(31), 6173-6178.
106. Liu Z., Hu J. , Sun Q., Chen L., Feng X., Zhao Y. , Mussel-inspired multifunctional coating for enhancing the UV-resistant property of polypropylene fibers, *Macromol. Res.*, **2017**, *25*(5), 431-438.
107. Oh C. E., Park Y. H., Kim S., Lim D., Park S. Y., In I., Photocatalytic activity of titanium dioxide nanoparticles linked on chemically reduced graphene oxide through mussel-inspired chemistry, *Chem. Lett.*, **2015**, *44*(8), 1068-1070.
108. Kim S. M., Park Y. H., Seo S. W., Park C. P., Park S.Y., In I., Mussel-inspired immobilization of catalysts for microchemical applications, *Adv. Mater. Interf.*, **2015**, *2*(11), 1500174.
109. Jeong C. J., In. I., Park S.Y., Facile preparation of metal nanoparticle-coated polystyrene beads by catechol conjugated polymer, *Surf. Interf. Anal.*, **2015**, *47*, 253-258.
110. Wang G., Huang X., Jiang P., Mussel-inspired fluoro-polydopamine functionalization of titanium dioxide nanowires for polymer nanocomposites with significantly enhanced energy storage capability, *Sci. Rep.*, **2017**, *7*, 43071; doi: 10.1038/srep43071.
111. Zheng X., Zhang J., Wang J., Qi X., Rosenholm J. M., Cai K., Polydopamine coatings in confined nanopore space: Toward improved retention and release of hydrophilic cargo, *J. Phys. Chem.* C., **2015**, *119*(43), 24512-24521.
112. Shi D., Zhang L., Shen J., Li X., Chen M., Akashi M., Fabrication of rod-like nanocapsules based on polylactide and 3,4-dihydroxyphenylalanine for a drug delivery system, *RSC Adv.*, **2015**, *5*(125), 103414-103420.
113. Zhang J., Cheah Y. S., Santhanakrishnan S., Neoh K. G., Chal C. L. L., Methoxy group substitution on catechol ring of dopamine facilitates its polymerization and formation of surface coatings, *Polymer.,* **2017**, *116*, 5-15.
114. Wu C., Zhang G., Xia T., Li Z., Zhao K., Deng Z., Guo D., Peng B., Bioinspired synthesis of polydopamine/Ag nanocomposite particles with antibacterial activities, *Mater. Sci. Eng. C Mater. Biol. Appl.*, **2015**, *55*, 155-165.
115. Wang Z., Ou J., Wang Y., Xue M., Wang F., Pan B., Li C., Li W., Anti-bacterial superhydrophobic silver on diverse substrates based on the mussel-inspired polydopamine, *Surf. Coat. Technol.*, **2015**, *280*, 378-383.
116. Xu Z., Miyazaki K., Hori T., Fabrication of polydopamine-coated superhydrophobic fabrics for oil/water separation and self-cleaning, *Appl. Surf. Sci.*, **2016**, *370*, 243-251.
117. Saito Y., Yabu H., Synthesis of poly(dihydroxystyrene-block-styrene) (PDHSt-b-PSt) by the RAFT process and preparation of organic-solvent-dispersive Ag NPs by automatic reduction of metal ions in the presence of PDHSt-b-PSt, *Chem. Commun.*, **2015**, *51*, 3743-3746.
118. Saito Y., Higuchi T., Jinnai H., Hara M., Nagano S., Matsuo Y., Yabu H., Silver nanoparticle arrays prepared by in situ automatic reduction of silver ions in mussel-inspired block copolymer films, Macromol. *Chem. Phys.*, **2016**, *217*, 726-734.
119. Tang J., Shi Z., Berry R. M., Tam K. C., Mussel-inspired green metallization of silver nanoparticles on cellulose nanocrystals and their enhanced catalytic reduction of 4-nitrophenol in the presence of β-cyclodextrin, *Ind. Eng. Chem. Res.*, **2015**, *54*(13), 3299-3308.
120. Lu Z., Xiao J., Wang Y., Meng M., In situ synthesis of silver nanoparticles uniformly distributed on polydopamine-coated silk fibers for antibacterial application, *J. Colloid Interf. Sci.*, **2015**, *452*, 8-14.

121. GhavamiNejad A., Unnithan A. R., . Sasikala A. R. K, Samarikhalaj M., Thomas R. G., Nasseri Y. Y. Jeong S., Murugesan P., Wu D., Park C. H., Kim C. S., Mussel-inspired electrospun nanofibers functionalized with size-controlled silver nanoparticles for wound dressing application, *ACS Appl. Mater. Interfaces*, **2015**, *7*(22), 12176-12183.
122. GhavamiNejad A., Aguilar L. E., Ambade R. B., Lee S.-H. S., Park C. H., Kim C. S., Immobilization of silver nanoparticles on electropolymerized polydopamine films for metal implant applications, Colloids and Interface Science Communications., **2015**, *6*, 5-8.
123. Nguyen H.-L., Jo Y. K., Cha M., Cha Y. J., Yoon D. K., Sanandiya N. D., Prajatelistia E., Oh X. D., Hwang D. S., Mussel-inspired anisotropic nanocellulose and silver nanoparticle composite with improved mechanical properties, electrical conductivity and antibacterial activity, *Polymers.,* **2016**, *8*(102), 13p; doi:10.3390/polym8030102.
124. Wu K., Yang Y., Zhang Y., Deng J., Lin C., Antimicrobial activity and cytocompatibility of silver nanoparticles coated catheters via a biomimetic surface functionalization strategy, *Intern. J. Nanomed.*, **2015**, *10*, 7241-7252.
125. Hu Y., Wang D., Li G., Mussel inspired redox surface for one step visual and colorimetric detection of Hg^{2+} during the formation of Ag@DOPA@Hg nanoparticles, *Anal. Methods* **2015**, *7*(15), 6103-6108.
126. Fu L., Lai G., Jia B., Yu A., Preparation and electrocatalytic properties of polydopamine functionalized reduced graphene oxide-silver nanocomposites, *Electrocatalysis.,* **2015**, *6*, 72-76.
127. Sajitha M., Vindhyasarumi A., Gopi A. and Yoosaf K., Shape controlled synthesis of multi-branched gold nanocrystals through a facile one-pot bifunctional biomolecular approach, *RSC Adv.*, **2015**, *5*(119), 98318-98324.
128. Roy A. K., Park S. Y., In I., Mussel-inspired synthesis of boron nitride nanosheet-supported gold nanoparticles and their application for catalytic reduction of 4-nitrophenol, *Nanotechnology.,* **2015**, *26*(10), 105601.
129. Zhou J., Wang P., Wang C., Goh Y. T., Fang Z., Messersmith P. B., Duan H., Versatile core-shell nanoparticle@metal-organic framework nanohybrids: Exploiting mussel-inspired polydopamine for tailored structural integration, *ACS Nano.,* **2015**, *9*(7), 6951-6960.
130. Wang C., Zhou J., Wang P., He W., Duan H., Robust nanoparticle-DNA conjugates based on mussel-inspired polydopamine coating for cell imaging and tailored self-assembly, *Bioconjugate Chem.*, **2016**, *27*(3), 815-823.
131. Jing Y., Yuan X., Yuan Q., He K., Liu Y., Lu P., Li H., Li B., Zhan H., Li G., Determination of nicotine in tobacco products based on mussel-inspired reduced graphene oxide-supported gold nanoparticles. *Sci. Rep.* **2016**, *6*, 29230; doi: 10.1038/srep29230 (2016).
132. Fu L., Yu A., Electroanalysis of dopamine using reduced graphene oxide-palladium nanocomposites, *Nanoscience and Nanotechnology Letters.,* **2015**, *7*(2), 147-151.
133. Xi J., Xiao J., Xiao F., Jin Y., Dong Y., Jing F., Wang S., Mussel-inspired functionalization of cotton for nano-catalyst support and its application in a fixed-bed system with high performance. *Sci. Rep.*, **2016**, *6*, 21904; doi: 10.1038/srep21904 (2016).
134. Zeng T., Zhang H., He Z., Chen J., Song S., Mussel-inspired approach to constructing robust cobalt-embedded N-doped carbon nanosheet toward enhanced sulphate radical-based oxidation. *Sci. Rep.*, **2016**, *6*, 33348; doi: 10.1038/srep33348 (2016).
135. Bai Y.,. Chang C.-C, Choudhary U., Bolukbasi I., Crosby A. J., Emrick T., Functional droplets that recognize, collect, and transport debris on surfaces, *Sci. Adv.*, **2016**, *2*(10), e1601462. DOI:10.1126/sciadv.1601462
136. Sun H., Ai M., Zhu S., Jia X., Cai Q., Yang X., Polylactide-hydroxyapatite nanocomposites with highly improved interfacial adhesion via mussel-inspired polydopamine surface modification, *RSC Adv.*, **2015**, *5*(116), 95631-95642.
137. Wan Q., Liu M., Tian J., Deng F., Zeng G., Li Z., Wang K., Zhang Q., Zhang X., Wei Y., Surface modification of carbon nanotubes by combination of mussel inspired chemistry and SET-LRP, *Polym. Chem.*, **2015**, *6*(10), 1786-1792.
138. Wan Q., Liu M., Tian J., Deng F., Dai Y., Wang K., Li Z., Zhang Q., Zhang X., Wei Y., Toward the development of versatile functionalized carbon nanotubes, *RSC Adv.* **2015**, *5*(48), 38316-38323.

139. Wan Q., Tian J., Liu M., Zeng G., Huang Q., Wang K., Zhang Q., Deng F., Zhang X., Wei Y., Surface modification of carbon nanotubes via combination of mussel inspired chemistry and chain transfer free radical polymerization, *Appl. Surf. Sci.*, **2015**, *346*, 335-341.
140. Wan Q., Tian J., Liu M., Zeng G., Li Z., Wang K., Zhang Q., Deng F., Zhang X., Wei Y., Mussel inspired preparation of highly dispersible and biocompatible carbon nanotubes, *RSC Advances.,* **2015**, *5*(32), 25329-25336.
141. Tian J., Xu D., Liu M., Deng F., Wan Q., Li Z., Wang K., He X., Zhang X., Wei Y., Marrying mussel inspired chemistry with SET-LRP: A novel strategy for surface functionalization of carbon nanotubes, *J. Polym. Sci., Part A: Polym. Chem.*, **2015**, *53*, 1872-1879.
142. Zhang X., Zeng G., Tian J., Wan Q., Huang Q., Wang K., Zhang Q., Liu M., Deng F., Wei Y., PEGylation of carbon nanotubes via mussel inspired chemistry:Preparation, characterization and biocompatibility evaluation, *Appl. Surf. Sci.*, **2015**, *351*, 425-432.
143. Wan Q., Mao L., Liu M., Wang K., Zeng G., Xu D., Huang H., Zhang X., Wei Y., Towards development of a versatile and efficient strategy for fabrication of GO based polymer nanocomposites, *Polym. Chem.*, **2015**, *6*(40), 7211-7218.
144. Shi Y., Liu M., Wang K., Deng F., Wan Q., Huang Q., Fu L., Zhang X., Wei Y., Bioinspired preparation of thermo-responsive graphene oxide nanocomposites in an aqueous solution, *Polym. Chem.*, **2015**, *6*(32), 5876-5883.
145. Fu L., Shi Y., Wang K., Zhou P., Liu M., Wan Q., Tao L., Zhang X., Wei Y., Biomimic modification of graphene oxide, *New J. Chem.*, **2015**, *39*(10), 8172-8178.
146. Luo J., Zhao F., Fei X., Liu X., Liu J., Mussel inspired preparation of polymer grafted graphene as a bridge between covalent and noncovalent methods, *Chem. Eng. J.*, **2016**, *293*, 171-181.
147. Zhang X., Nan X., Shi W., Sun Y., Su H., He Y., Liu X., Zhang Z., Ge D., Polydopamine-functionalized nanographene oxide: a versatile nanocarrier for chemotherapy and photothermal therapy, Nanotechnology., **2017**, *28*(29), 295102.
148. Miao J., Liu H., Li W., Zhang X., Mussel-inspired polydopamine-functionalized graphene as a conductive adhesion promoter and protective layer for silver nanowire transparent electrodes, *Langmuir.,* **2016**, *32*(21), 5365-5372.
149. Liu J., Wang T., Wang J., Wang E., Mussel-inspired biopolymer modified 3D graphene foam for enzyme immobilization and high performance biosensor, *Electrochim. Acta .,* **2015**, *161*, 17-22.
150. Meng F., Wei W., Chen J., Chen X., Xu X., Jiang M., Wang Y., Lu J., Zhou Z., Growth of Fe3O4 nanosheet arrays on graphene by a mussel-inspired polydopamine adhesive for remarkable enhancement in electromagnetic absorptions, *RSC Adv.*, **2015**, *5*(122), 101121-101126.
151. Wang X. , Hu N. , Zeng F. , Wang L. , Yin H., Hou C., Zhou L. , Zhu H. , Mussel-inspired surface modification of magnetic@graphite nanosheets composite for efficient Candida rugosa lipase immobilization, *J. Ind. Microbiol. Biotechnol.,* **2015**, *42*(5), 723-734.
152. Liu X., Men C., Gao P., Zhuang S., Tang H., Bao Z., Improved cycling performance of sulfur nanoparticles with a mussel inspired polydopamine coating, *RSC Adv.*, **2016**, *6*(3), 1902-1906.
153. Kim B. J., Kim S., Oh D. X., Masic A., Cha H. J., Hwang D. S., Mussel-inspired adhesive protein-based electrospun nanofibers reinforced by Fe(III)-DOPA complexation, *J. Mater. Chem.*, B, **2015**, *3*, 112-118.
154. Kim B. J., Cheong H., Hwang B. H., Cha H. J., Mussel-inspired protein nanoparticles containing iron(III)-DOPA complexes for pH-responsive drug delivery, Angew. *Chem. Int. Ed.*, **2015**, *54*, 1-6.
155. Han J., Park W., Park S.-j., Na. K., Photosensitizer-conjugated hyaluronic acid-shielded polydopamine nanoparticles for targeted photomediated tumor therapy, *ACS Appl. Mater. Interfaces.,* **2016**, *8*(12), 7739-7747.
156. Hafner D., Ziegler L., Ichwan M., Zhang T., Schneider M., Schiffmann M., Thomas C., Hinrichs K., Jordan R., Amin I., Mussel-inspired polymer carpets: direct photografting of polymer brushes on polydopamine nanosheets for controlled cell adhesion, *Adv. Mater.*, **2015**, 6. DOI:10.1002/adma.201504033.

157. Liu M., Ji J., Zhang X., Zhang X., Yang B., Deng F., Li Z., Wang K., Yang Y., Wei Y., Self-polymerization of dopamine and polyethyleneimine: novel fluorescent organic nanoprobes for biological imaging applications, *J. Mater. Chem.,* B **2015**, *3*(17), 3476-3482.
158. Zhao C., Zuo F., Liao Z., Qin Z., Du S., Zhao Z., Mussel-inspired one-pot synthesis of a fluorescent and water-soluble polydopamine-polyethyleneimine copolymer, Macromol. *Rapid Commun.*, **2015**, *36*, 909-915.
159. Jiang J., Wan W., Ge L., Bu S., Zhong W., Xing M., Mussel-inspired nanofibrous sheet for suture-less stomach incision surgery, *Chem. Commun.*, **2015**, *51*(41), 8695-8698.
160. Lee M., Park C., Lee H., Kim H., Kim S. Y., In I., Kim B., Remarkably enhanced adhesion of coherently aligned catechol-terminated molecules on ultraclean ultraflat gold nanoplates, *Nanotechnology.,* **2016**, *27*(47), 475705.
161. Zeng G., Liu M., Liu X., Huang Q., Xu D., Mao L., Huang H., Deng F., Zhang X., Wei Y., Mussel inspired preparation of MoS2 based polymer nanocomposites: The case of polyPEGMA, *Appl. Surf. Sci.*, **2016**, *387*, 399-405.
162. Ghadban A., Ahmed A. S., Ping Y., Ramos R., Arfin N., Cantaert B., Ramanujan R. V., Miserez A., Bioinspired pH and magnetic responsive catechol-functionalized chitosan hydrogels with tunable elastic properties, *Chem. Commun.*, **2016**, *52*, 697-700.
163. Jia Y.-G., Zhu X. X., Nanocomposite hydrogels of LAPONITE® mixed with polymers bearing dopamine and cholic acid pendants, *RSC Adv.*, **2016**, *6*(27), 23033-23037.
164. Liu Y., Meng H., Qian Z., Fan N., Choi W., Zhao F., Lee B. P., A moldable nanocomposite hydrogel composed of a mussel-inspired polymer and a nanosilicate as a fit-to-shape tissue sealant, *Angew. Chem. Int. Ed. Engl.,* **2017**, *56*(15), 4224-4228.
165. Han L., Lu X., Liu K., Wang K., Fang L., Weng L.-T., Zhang H., Tang Y., Ren F., Zhao C., Sun G., Liang R., Li Z., Mussel-inspired adhesive and tough hydrogel based on nanoclay confined dopamine polymerization, *ACS Nano.,* **2017**, *11*(3), 2561-2574.
166. Han L., Lu X., Wang M., Gan D., Deng W., Wang K., Fang L., Liu K.,. Chan C. W, Tang Y., Weng L. T., Yuan H., A mussel-inspired conductive, self-adhesive, and self-healable tough hydrogel as cell stimulators and implantable bioelectronics, *Small.,* **2017**, *13*(2), 1601916.
167. GhavamiNejad A., SamariKhalaj A., Aguilar L. E., Park C. H., Kim C. S., pH/NIR light-controlled multidrug release via a mussel-inspired nanocomposite hydrogel for chemo-photothermal cancer therapy, *Sci. Rep.*, **2016**, *6*, 33594; doi: 10.1038/srep33594.
168. Yin X.-n., Wang J., Zhou J.-j., Li L., Mussel-inspired modification of Microporous polypropylene membranes for functional catalytic degradation, *Chin. J. Polym. Sci.*, **2015**, *33*(12), 1721-1729.
169. Du Y., Yang H.-C., Xu X.-L., Wu J., Xu Z.-K., Polydopamine as a catalyst for thiol coupling, *Chem Cat Chem.,* **2015**, *7*(23), 3822-3825.
170. Zhang C., Yang H.-C, Wan L.-S., Liang H.-Q., Li H., Xu Z.-K., Polydopamine-coated porous substrates as a platform for mineralized β-FeOOH nanorods with photocatalysis under sunlight, *ACS Appl. Mater. Interfaces.,* **2015**, *7*(21), 11567-11574.
171. Yuan C., Chen J., Yu S., Chang Y., Mao J., Xu Y., Luo W., Zeng B. and Dai L., Protein-responsive assemblies from catechol-metal ion supramolecular coordination, *Soft Matter.,* **2015**, *11*(11), 2243-2250.